CHALMERS

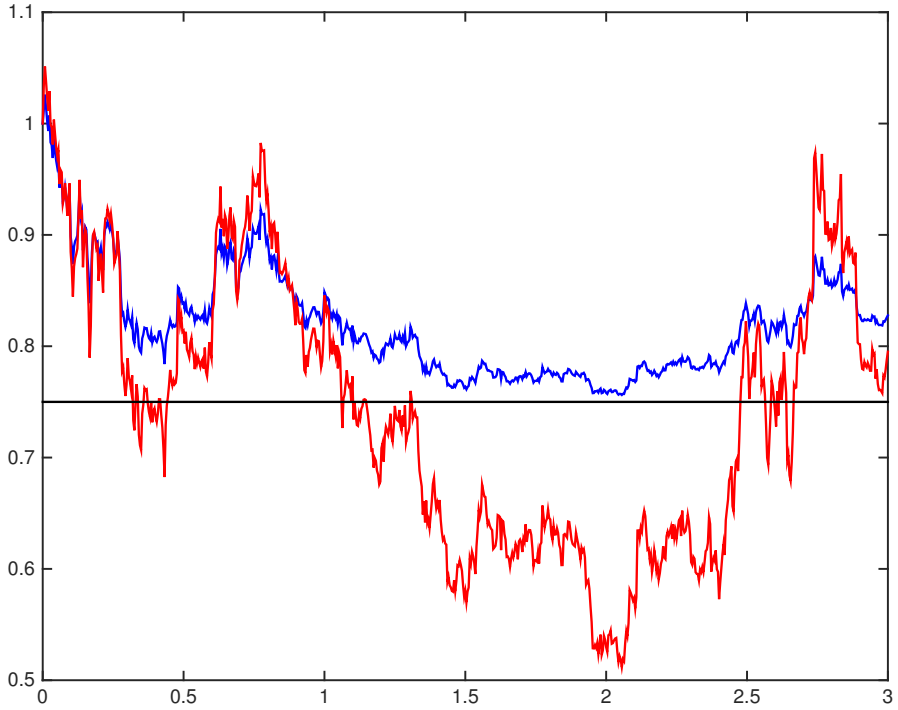

Portfolio Insurance Strategies in an Extended Black-Scholes Framework Including Jumps in Asset Prices

Master's Thesis in Engineering Mathematics and Computational Science

PHILIPPE KLINTEFELT COLLET

Department of Mathematical Sciences
Chalmers University of Technology
Gothenburg, Sweden 2014
Master's Thesis 2014:2

Abstract

The Constant Proportion Portfolio Insurance (CPPI) and Option Based Portfolio Insurance (OBPI) strategies are examined and evaluated in an extended Black-Scholes framework including jumps in asset prices, stochastic volatility, and stochastic interest rate and bond prices. The Kou model (an exponential Lévy model) was used to model the dynamics of the risky assets. Interest rate was modelled according to the Vasicek model (an Ornstein-Uhlenbeck model). The method of empirical characteristic exponent was applied in order to calibrate the Kou model towards real-world financial data. By means of the Monte Carlo method, the portfolio strategies were analysed through simulation.

If was found that in calmer market conditions, the OBPI strategy slightly outperforms the CPPI. As the CPPI has negligible risk of default in those market conditions, it can be used as a replacement for the OBPI in the absence of a liquid options market. In highly volatile markets, on the other hand, the CPPI clearly outperforms the OBPI, especially when the time to maturity is relatively short. However, as the intensity and sizes of jumps in asset prices increase, the CPPI can reach important levels of risk of default.

The risk of default as a function of the multiplier in the CPPI strategy is examined in detail, using model parameters estimated from MSFT, BMW and AZN stocks as well as SNP500, SX5E and NIKKEI225 indices.

Acknowledgements

I would like to extend my most sincere thanks to Prof. Patrik Albin for supervising my work, his support and constructive ideas, the very nice conversations in his office, and for having faith in my efforts.

I would also like to direct my gratitude towards some of the staff at Chalmers and École Polytechnique who have been particularly influential on me throughout the years: Prof. Jana Madjarova at Chalmers for taking me as her pupil even as I was still a young high school student; Prof. Martin Cederwall, Prof. Christian Forssén and Prof. Måns Henningson at Chalmers for helping me see the beauty and wonder of physics; and Prof. Peter Tankov at École Polytechnique for introducing me to the world of mathematical finance.

Lastly, I would like to express my dearest love to my wonderful parents and brother. You have, each in your own particular way, provided me with incredible support and motivation throughout my entire life. Without you, I'm not sure what I would be.

Philippe Klintefelt Collet
Göteborg, December 13, 2014

Contents

1

Introduction

In the light (or darkness) of the still recent financial crisis, the issue of portfolio insurance has become increasingly important to many investors [2]. The term *portfolio insurance* is understood as a trading strategy which allows for the guarantee of a certain minimal portfolio value at maturity, while keeping a fraction of the wealth invested into risky assets. The purpose of such strategies is to provide protection in falling markets while still preserving some exposure to potential positive market moves. Two very popular such strategies are the Constant Proportion Portfolio Insurance (CPPI) strategy, which revolves around dynamic rebalancing of the portfolio contents according to a certain scheme, and the Option Based Portfolio Insurance (OBPI) strategy, which revolves around the usage of put options to protect a fraction of the risky investment: These two strategies are introduced in Section 1.1 and Section 1.2, respectively.

The literature includes various studies of the relative performance of these two strategies, but most such work is of theoretical nature. For example, El Karoui, Jeanblanc and Lacoste proved in 2005 the optimality of the OBPI strategy within the framework of complete, arbitrage free, frictionless markets, when an expected CRRA utility function is maximized [6]. Bertrand and Prigent, in turn, conducted their 2003 study within the basic Heston model. They were able to show that by correcting the Black-Scholes assumptions by introducing stochastic volatility, the expected return of the OBPI strategy increases while the expected return of the CPPI strategy slightly decreases. All while the standard deviation, skewness, and kurtosis of both strategies are affected [1].

However, such results often have limited practical applicability. For instance, it may be shown that under the Black-Scholes assumptions, as soon as the drift of the risky asset is higher than the risk-less interest rate, the expected return of the CPPI portfolio can be increased indefinitely without any risk of the portfolio value dropping below the guaranteed amount (see Section 1.1.1). Throughout this text it will become apparent that such shortcomings stem from the negligence of some of the most important risks

that portfolio insurance strategies are subjected to, for example those related to jumps in the price of the risky asset.

In this context, the focus and goal of the present text is to approach analysis of the performance and behaviour of the portfolio insurance strategies in a way that is more applicable to the real world. A first step in this direction is to extend the Black-Scholes framework by introduction of jumps in asset prices, stochastic volatility, as well as stochastic interest rates. Once a working set of models is established, the parameters of the models may be estimated by calibration from real-world financial data.

1.1 Constant Proportion Portfolio Insurance

The Constant Proportion Portfolio Insurance (CPPI) strategy dates back to the late 1980:s when it was introduced by Perold in 1986 for fixed-income instruments and Black and Jones in 1987 for equity instruments [see 3, 12]. It is a dynamic investment strategy, as it requires the manager to readjust the portfolio over time. As a portfolio insurance strategy, its purpose is to provide the investor with an exposure to the upside potential of risky assets while providing a pre-determined capital guarantee against downward market movements — in other words, guaranteeing that the portfolio value at maturity will be greater than or equal to a certain lower bound (called the *floor*) while maintaining the opportunity to profit from positive market movers.

The principle of the strategy revolves around the notion of a *cushion*, defined as the difference between the current portfolio value and the floor. As the strategy is implemented, first of all the floor is determined as a representation of the minimum portfolio value that the investor can accept at maturity. Thereafter, an amount of wealth equal to a predetermined multiple $m > 1$ of the cushion is allocated to the risky asset, while the remainder is invested in the riskless asset, such as riskless bonds or equivalent. Note that this means that as long as the portfolio value is greater than the floor, a non-zero amount of wealth will be invested in the risky asset and the total investment in the riskless asset will be less than than the floor, since $m > 1$. As the floor and the multiplier are predetermined as functions of the investor's risk tolerance, they are exogenous to the model. The definition of the model implies, in particular, that as the markets move down and the portfolio value approaches the floor, the exposure to the risky asset is decreased and the exposure to the riskless asset increased (vice-versa as the markets move up).

A higher multiple means that the investor will participate to a greater extent in sustained increases in the risky asset, but also see the portfolio reach the floor faster when the markets move down as well as be more vulnerable to very sudden downward market movements. Multiplier values between 2 and 5 are common [5].

1.1.1 CPPI under continuous Black-Scholes model

As previously described, the CPPI strategy is a self-financing strategy whose goal is to leverage the returns of a risky asset (typically a traded fund or index) through dynamic

trading, while guaranteeing a fixed amount at N maturity T. To achieve this, the portfolio manager shifts his/her position between the risky asset S_t and a *reserve* asset B_t which is typically a bond. For simplicity, the reserve asset will be modelled as a zero-coupon bond with maturity T and nominal N. The exposure to the risky asset is a function of the *cusion* C_t, defined as [5, p. 380]

$$C_t = V_t - B_t. \tag{1.1}$$

At any date t

(1) if $V_t > B_t$, the exposure to the risky asset (wealth invested into the risky asset) is given by $mC_t \equiv m(V_t - B_t)$, where $m > 1$ is a constant multiplier.

(2) if $V_t \leq B_t$, the entire portfolio is invested in the zero-coupon bond.

For now, the interest rate r is assumed constant and the underlying asset to follow a Black-Scholes model

$$\frac{dS_t}{S_t} = \mu dt + \sigma dW_t.$$

It then follows from the definition of the strategy that the cushion also satisfies the Black-Scholes stochastic differential equation

$$\frac{dC_t}{C_t} = (m\mu + (1-m)r)dt + m\sigma dW_t,$$

which is solved explicitly by

$$C_T = C_0 \exp\left(rT + m(\mu - r)T + m\sigma W_T - \frac{m^2\sigma^2 T}{2}\right),$$

and hence Equation (1.1) gives

$$V_T = N + (V_0 - Ne^{-rT}) \exp\left(rT + m(\mu - r)T + m\sigma W_T - \frac{m^2\sigma^2 T}{2}\right). \tag{1.2}$$

This means that in the context of the Black-Scholes model with continuous trading, the CPPI strategy is equivalent to taking a long position in a zero-coupon bond with nominal N to guarantee the capital at maturity and investing the remaining sum into a (fictitious) risky asset which has m times the excess return and m times the volatility of S and is perfectly correlated with S.

1.1.2 Price jumps and "gap risk"

As seen in formula (1.2), in the Black-Scholes model with continuous trading there is never any risk of going below the floor, regardless of the multiplier value. Even so, the expected return of a CPPI-insured portfolio is

$$E[V_T] = N + (V_0 - Ne^{-rT}) \exp(rT + m(\mu - r)T),$$

which leads to the paradoxical conclusion that in the Black-Scholes model, whenever $\mu > r$, the expected return of a CPPI portfolio can be increased indefinitely and without risk, simply by increasing the multiplier.

Yet there is a widely recognized risk of breaching the floor, known as "gap risk", that has to be taken into account by CPPI managers: There is a non-zero risk that, during a sudden downward market movement, the fund manager will not have the time to rebalance the portfolio, which then crashes through the floor. When this happens the issuer has to refund the difference, at maturity, between the actual portfolio value and the guaranteed amount N. It is therefore important for the issuer of the CPPI note to quantify and manage this so-called "gap risk".

Beyond the (widely documented) econometric issue of whether jumps in asset prices occur or not, liquidity may have a fundamental impact on the gap risk: oftentimes CPPI strategies are written on funds which may be thinly traded, leading to jumps in market prices due to liquidity effects. Since the volatility of V_t is proportional to m, the risk of such a losses increases with m. It is therefore clear why, in practice, the multiplier should be fixed by relating it to an acceptance threshold of some risk measure, such as probability of loss or maximum one-day loss [5].

1.2 Option Based Portfolio Insurance

The Option Based Portfolio Insurance (OBPI) strategy was first introduced by Leland and Rubinstein in 1976 [see 11]. In it's simplicity, it consists of buying a risky asset S, such as stocks or a financial index, while simultaneously buying a put option on it. In this way, the portfolio value at maturity T is guaranteed to be at least equal to the strike K of the put, no matter what the value of S is at maturity. From this definition, it may be obvious that the OBPI strategy fulfills the purpose of guaranteeing a certain given amount at maturity. But it turns out that, due to its definition, the OBPI strategy provides the possibility of portfolio insurance at every time up to maturity. However, there may, for various reasons, not always always be a put option on the the asset in question available on the market; in those cases either the put can be replicated by various means, or other hedging strategies — such as the CPPI strategy — may be chosen for implementation instead. More on this strategy is covered in the light of portfolio simulations in Chapter 4, which in turn rest on the put price calculations presented in Appendix B.

1.3 Stylized facts

Some of the imperfections of the Black-Scholes model have already been touched upon. However, it is effort well spent to re-summarize and elaborate a little on a few relevant phenomena of the real-world financial markets. So-called *stylized facts* are generally accepted empirical observations which, from a general point of view, hold true within the financial markets. A few such stylized facts are elaborated on in this section, as they

are particularly relevant to the hedging portfolio strategies that will later come under investigation.

1.3.1 Skewness and leptokurtosis of the distribution of returns

Overwhelming evidence shows that the skewness and kurtosis of stocks return differ, often significantly, from the Gaussian distribution [15]. The Gaussian distribution possesses skewness and kurtosis values of 0 and 3, respectively. In most cases, real-world returns display slightly negative skewness and are leptokurtic (kurtosis greater than 3) [4]. The leptokurtic property, also known as "fat tails" property, implies that the tails of the distribution of historical returns are thicker than those predicted by the Gaussian distribution. In particular, this means that extreme market events occur more often in the real world than is predicted within the Black-Scholes framework. This has has important implications for, among other things, option pricing.

1.3.2 Volatility clustering

Another stylized fact of financial time series is the presence of *volatility clustering*. Simply speaking, volatility clustering refers to the fact that there are periods of time when volatility is relatively high and periods of time when volatility is relatively low. This is another feature that is not taken into account by the Brownian motion of the Black-Scholes model. To model volatility clustering, stochastic volatility must be used — i.e. volatility must be modelled as a stochastic process.

1.3.3 Discontinuity of trajectories

In the Brownian motion model used within the Black-Scholes framework, trajectories are continuous. However, as is widely observed in the financial markets, continuity is not a very realistic assumption [15]. Even though stock quotes may appear continuous on large time-scales, discontinuities will often become apparent on smaller ones, such as intra-day time-scales. There are many reasons for why the stock market displays discontinuities; a simple one could be discrepancies between the closing and opening prices, especially if some important news (positive or averse) have become public during the market's closure.

2

Model Setup

The classical Black-Scholes framework has some serious limitations, as was pointed out in Chapter 1. To circumvent these limitations, it is necessary to change the assumptions made on the behaviour of the financial assets. A first step in this direction is to introduce jumps into the model of the stock price evolution. This first extension, as will become apparent, is the key to quantifying the default risk of the CPPI strategy. Furthermore, in the light of the well-observed volatility clustering phenomena, stochastic volatility modelling is pursued. Interest rate modelling using the Vasicek model is investigated, which among other things, provides the bond prices some dynamics.

For simplicity it is assumed, as in the Black-Scholes model, that the financial market consists of only two assets: the risky (e.g. stocks/index) and the risk-less (e.g. bond/gilt) asset.

2.1 Stock price dynamics and stochastic volatility

The dynamics of the risky asset $(S)_{t\geq 0}$ is assumed to be described by the SDE

$$\frac{dS_t}{S_{t-}} = dZ_t, \tag{2.1}$$

where $(Z)_{t\geq 0}$, in the general case, is a possibly discontinuous driving process modelled as a semimartingale. From here on, Z_t will be the exponential Lévy process (see Equation (2.3) below). Without loss of generality it can be assumed $S_0 = 1$, as this can always be achieved through normalization. The SDE (2.1) can be solved as a Doléans-Dade exponential [13, pp. 159-160], and has the explicit solution

$$S_t = \exp\left(Z_t - \frac{1}{2}\int_0^t \sigma_s^2 ds\right) \cdot \prod_{0\leq s\leq t, \Delta Z_s \neq 0} (1 + \Delta Z_s) e^{-\Delta Z_s}, \tag{2.2}$$

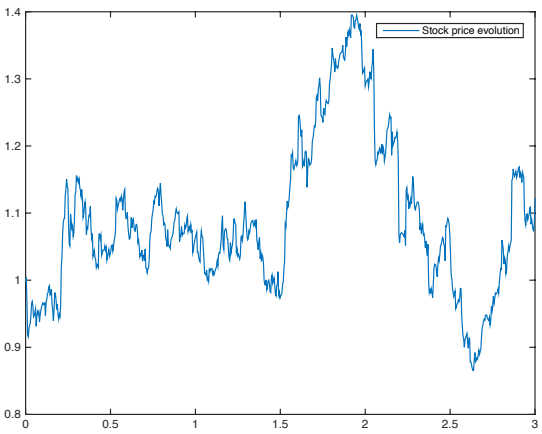

(a) Stock price trajectory under stochastic volatility as a function of time (years).

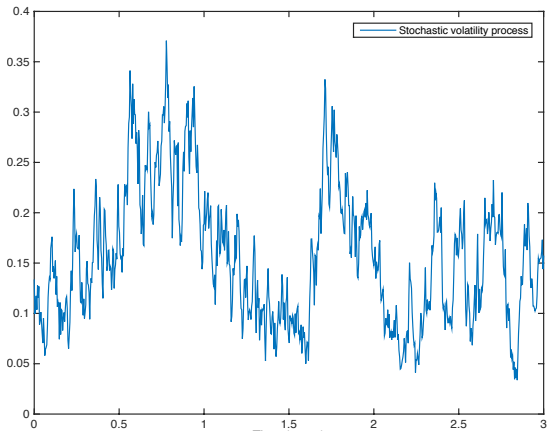

(b) Trajectory of a stochastic volatility process with parameters $k = 20$, $\theta = 0.15$ and $\delta = 0.9$, as a function of time (years).

Figure 2.1: Examples of trajectories of stock price (left) and stochastic volatility (right).

where ΔZ_t are jump occurrences in Z_t and σ_t^2 is the volatility of its Brownian component. From Equation (2.2) it becomes obvious that the assumption $\Delta Z_t \geq -1$ must be made in order to prevent negative prices.

The process Z_t is modelled as a jump-diffusion, and is described by

$$Z_t = \mu t + \sigma_t W_t + \sum_{i=1}^{N_i} Y_i, \tag{2.3}$$

where μt represents the deterministic trend, $\sigma_t W_t$ is the Brownian part, and last term is the *jump part*. Here, $(Y_i)_{i \in N_t}$ is a family of i.i.d. random variables and N_t is a Poisson process with intensity λ, meaning that the jump part is in fact a so-called compound Poisson process. The so-called *Kou model* will be applied, by which $(Y_i)_{i \in N_t}$ is distributed according to the asymmetrical Laplace distribution (also known as the *double exponential distribution*) with parameters (p, η_+, η_-): p being the probability that a given jump is negative, and η_+ and η_- being the characteristic lengths of, respectively, positive and negative jumps.

To account for volatility clustering, volatility is modelled stochastically according to the SDE

$$d\sigma_t = k(\theta - \sigma_t)dt + \delta\sqrt{\sigma_t}dW_t.$$

This model is similar to the Vasicek model used for modelling bonds (see Section 2.2): θ represents the long-run average and k the speed of adjustment. $\delta < 2k\theta$ is assumed in order to prevent negative values.

An example of the stochastic evolution of the stock price under the Kou-model and of stochastic volatility may be seen in Figure 2.1

2.1.1 Numerical implementation

In order to implement the model numerically, time is discretized into a finite set of times $\{t_i\}_{i=1}^N$ where $t_i < t_{i+1}$ for all $0 \leq i < N$, $t_0 = 0$, and $t_N = T$. These times are interpreted as trading dates. By using an evenly spaced time-lattice $t_i = \frac{iT}{N}$ with N sufficiently large, it is reasonable to approximate the stochastic volatility σ_t as constant within each of the time intervals $[t_i, t_{i+1})$. Starting from the initial value σ_0, the volatility is then calculated as

$$\sigma_{t_i} = \sigma_{t_{i-1}} + k(\theta - \sigma_{i-1})(t_i - t_{i-1}) + \delta\sqrt{\sigma_{t_{i-1}}}\sqrt{t_i - t_{i-1}}N(0,1),$$

where $N(0,1)$ is a standard normal random variable.

The process Z_t is then computed as

$$Z_{t_i} = Z_{t_{i-1}} + \mu(t_i - t_{i-1}) + \sigma_{t_{i-1}}\sqrt{t_i - t_{i-1}}N(0,1) + \Delta_i, \tag{2.4}$$

where Δ_i represents the jump part $\Delta_i(\sum_{i=1}^{N_i} Y_i)$. As the jump part follows the Kou scheme, Δ_i is calculated as follows:

(1) The jump count $N_i \sim \text{Poi}(\lambda(t_i - t_{i-1}))$ is generated.

(2) If $N_i = 0$ then $\Delta_i = 0$, else $\{Y_i\}_{i=1}^{N_i}$ are generated according to the Laplace law with parameters (p, η_+, η_-) and added to Z_{t_i}.

2.2 Dynamics of the riskless asset

The riskless asset dynamics are modelled using the so-called Vasicek model: In this framework, the short-term interest rate follows the Ornstein-Uhlenbeck process

$$dr_t = a(b - r_t)dt + \sigma dW_t,$$

where, for simplicity, the Brownian motion W_t is assumed independent of the Brownian motion used in the Lévy process presented in Section 2.1. The parameters of this SDE may be interpreted in the following way

b is the long-run interest rate

a is a factor characterizing the speed at which trajectories of the interest rate regroup around the long-run value

σ is a (constant) volatility parameter

The SDE is of Langevin type and admits the closed-form solution [9, p. 128]

$$r_t = r_0 e^{-at} + b(1 - e^{-at}) + \sigma e^{-at}\int_0^t e^{as}dW_s.$$

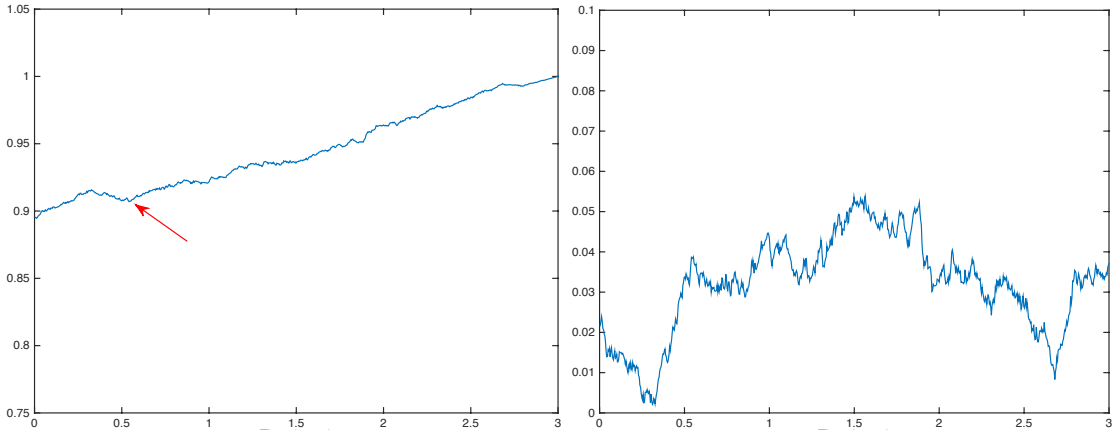

(a) Price dynamics of the zero coupon bond under stochastic interest rate as a function of time (years). Note how changes in interest rate causes the price to drop even as time to maturity decreases (indicated by the arrow).

(b) Trajectory of the stochastic interest rate under the Vasicek model as a function of time (years), with parameters $a = 2$, $b = 0.04$ and $\sigma = 0.02$.

Figure 2.2: Bond price (left) and interest rate (right) dynamics generated using the Vasicek model.

The solution suggests that trajectories of r_t will regroup around the mean value b and variance $\frac{\sigma^2}{2a}$, as $t \to \infty$.

Provided the dynamics of the interest rate r_t, the price $B_t(T)$ at time t of the zero-coupon bond with maturity T may be calculated as

$$\begin{aligned} B_t(T) &= E[\exp\left(-\int_t^T r_s ds\right) \mid F_t] \\ &= \exp\left(-b(T-t) + (b-r_t)\frac{1-e^{-a(T-t)}}{a} - \frac{\sigma^2}{4a^3}(1-e^{-a(T-t)})^2 \right. \\ &\qquad \left. + \frac{\sigma^2}{2a^2}(T-t-\frac{1-e^{-a(T-t)}}{a})\right) \end{aligned} \quad . \quad (2.5)$$

Examples of the evolution of the bond price and stochastic interest rate may be seen in Figure 2.2

2.2.1 Numerical implementation

Just as in Section 2.1.1, time is discretized into a finite set of times $\{t_i\}_{i=1}^N$ which are interpreted as trading dates. In order to avoid discretization errors, the dynamic interest rate r_t is computed from the closed form solution

$$r_t = r_{t_{i-1}} e^{-a(t_i - t_{i-1})} + b(1 - e^{-a(t_i - t_{i-1})}) + \sigma e^{-a(t_i - t_{i-1})} \int_{t_{i-1}}^{t_i} e^{as} dW_s,$$

where $\int_{t_{i-1}}^{t_i} e^{as} dW_s \sim \sqrt{\int_0^{t_i - t_{i-1}} e^{2as} ds} \cdot N(0,1)$ [9, p. 110]. The set of bond prices $\{B_{t_i}\}_{i=1}^N$ is then calculated using formula (2.5).

3

Model Calibration

The models presented in Chapter 2 hold the potential to represent the behaviour of their real-word counterparts. However, they need to be calibrated before any practical applicability is obtained. "Calibration" refers to the process of using real-world observations to give the various parameters in the models specific values.

The Kou model, used to simulate stock price dynamics, turns out to be difficult to calibrate using standard maximum likelihood estimations or least squares regression. So instead, calibration of the model is approached using the empirical characteristic function; by minimizing, with respect to the model parameters, the "distance" (in the sense of integration) between the characteristic exponent of the model, which can be found explicitly, and the so-called *empirical characteristic exponent*, the calibrated parameters are obtained.

The Vasicek model, on the other hand, is of simpler nature, and may be calibrated using maximum likelihood estimates. This is done in detail in Section 3.2.

3.1 Calibrating the Kou model

As of Section 2.1, the price of the risky asset follows an exponential Lévy model or, more specifically, the so-called Kou model. In this model the driving Lévy process has a non-zero Gaussian component and a Lévy density of the form

$$v(x) = \frac{\lambda(1-p)}{\eta_+} e^{-x/\eta_+} \mathbf{1}_{x>0} + \frac{\lambda p}{\eta_-} e^{-|x|/\eta_-} \mathbf{1}_{x<0}.$$

Here, λ is the total intensity of positive and negative jumps, p is the probability that a given jump is negative, and η_-, and η_+ are characteristic lengths of, respectively, negative and positive jumps.

To determine the components of the parameter vector $\theta = (\mu, \sigma, \lambda, p, \eta_+, \eta_-)$, the method of empirical characteristic function is applied [see 16].

Courtesy of this method, θ is obtained my minimizing the distance-integral

$$\int_{-K}^{K} |\psi_\theta(u) - \hat{\psi}(u)|^2 w(u)\, du,$$

where

$$\hat{\psi}(u) = \frac{1}{t} \log \frac{1}{N} \sum_{k=1}^{N} e^{iuX_k}$$

is the so-called *empirical characteristic exponent*,

$$\psi_\theta(u) = -\frac{\sigma^2 u^2}{2} + i\mu u + \frac{\lambda p}{1 + iu\eta_-} + \frac{\lambda(1-p)}{1 - iu\eta_+} - \lambda$$

is the characteristic exponent of the Kou model [see 10], and $w(u)$ is a weight function. Here, the set $\{X_k\}_{k=1}^N$ is the dataset of log-returns used for calibration, and t is the period of these returns (e.g. $\sim \frac{1}{252}$ for daily returns using the unit 1 year, etc.).

Ideally, the weight function $w(u)$ should answer to the precision of $\hat{\psi}(u)$ as an estimate of $\psi_\theta(u)$ for every u, and therefore be chosen as the reciprocal of the variance of $\hat{\psi}(u)$:

$$\begin{aligned} w(u) &= \frac{1}{E[(\hat{\psi}(u) - E[\hat{\psi}(u)])\overline{(\hat{\psi}(u) - E[\hat{\psi}(u)])}]} \\ &\approx \frac{t^2 \phi_{\theta^*}(u)\overline{\phi_{\theta^*}(u)}}{E[(\hat{\phi}(u) - \phi_{\theta^*}(u))\overline{(\hat{\phi}(u) - \phi_{\theta^*}(u))}]}, \end{aligned}$$

where θ^* is the true parameter [5, p. 394]. However, this expression is not fruitful to deal with, as it depends on the unknown parameter vector θ and therefore cannot be computed. Since the return distribution is relatively close to Gaussian, the characteristic function of the weight w may be approximated with a Gaussian one

$$w(u) \approx \frac{e^{-\sigma_*^2 u^2}}{1 - e^{-\sigma_*^2 u^2}},$$

where $\sigma_*^2 = \mathrm{Var}(\{X_k\}_{k=1}^N)$ is the variance of the log returns data. The cut-off parameter K should be chosen based on tests with simulated data. Previous results show that the estimated parameter values are not very sensitive to this parameter for $K > 50$ [5, p. 394].

Examples of estimations of the parameters of the Kou model are displayed in Table 5.1. Figure 3.1 illustrates the goodness of fit achieved: The Kou model fits the smoothed returns density quite well and, in particular, the exponential tail decay appears to be a realistic assumption.

More comprehensive calibration results are presented in Chapter 5, which further refers to Appendix C. In Section D.1 in Appendix D, a `MATLAB` implementation of the calibration method can be found.

Series	μ	σ	λ	p	η_+	η_-
MSFT	0.1078	0.1129	133.0564	0.4594	0.0109	0.0112
BMW	0.3641	0.1582	374.7105	0.4428	0.0058	0.0086
NIKKEI225	0.1875	0.1664	94.7402	0.4473	0.0081	0.0091

Table 3.1: Kou model parameters estimated from MSFT and BMW stocks, and the NIKKEI225 index. The data spans 3 years, from 2 December 2011 to 30 November 2014.

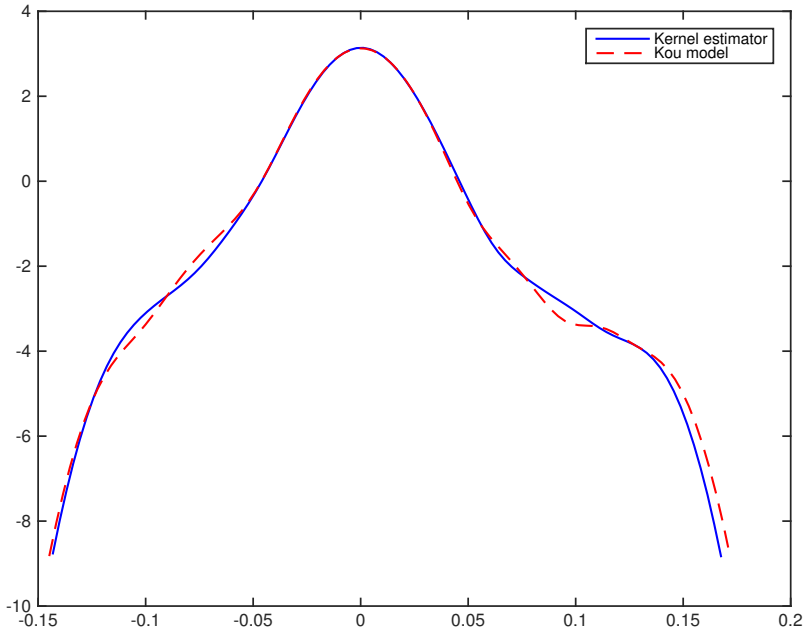

Figure 3.1: Logarithm of the density for MSFT time series. Solid line: Kernel density estimator applied directly on data. Dashed line: Kou model simulation with parameters estimated via empirical characteristic exponent.

3.2 Calibrating the Vasicek model

Recalling the Vasicek model, it's dynamic is of the form

$$dS_t = a(b - S_t)dt + \sigma dW_t \tag{3.1}$$

where a is the mean reversion rate, b the mean, and σ the volatility. If the difference $t_{i+1} - t_i = \delta$, then the exact solution to (3.1) may be written on the form:

$$dS_{t_{i+1}} = S_{t_i} e^{-a\delta} + b(1 - e^{-a\delta}) + \sigma \sqrt{\frac{1 - e^{-2a\delta}}{2a}} N_{0,1}, \tag{3.2}$$

where $N_{0,1}$ is a standard normal random variable. If, as will be assumed, observed data $\{S_i\}_{i=0}^n$, evenly spaced in time with a period of δ, is available, then calibration using *maximum likelihood estimates* is easily implemented.

3.2.1 Maximum likelihood function

The conditional density function is easily derived by combining Equation (3.2) with the normal probability density function:

$$f_{N_{0,1}} = \frac{1}{\sqrt{2\pi}} e^{-\frac{1}{2}x^2}.$$

The formula for the conditional probability density function of an observation S_{i+1} given a previous observation S_i (with time step δ between them), is given by

$$\begin{aligned} &f(S_{i+1}|S_i; a, b, \sigma) \\ &= \frac{1}{\sqrt{2\pi\hat{\sigma}^2}} \exp\left(-\frac{(S_i - S_{i-1}e^{-a\delta} - b(1 - e^{-a\delta}))^2}{2\hat{\sigma}^2} \right), \end{aligned} \tag{3.3}$$

where

$$\hat{\sigma}^2 = \sigma^2 \frac{1 - e^{-2a\delta}}{2a}.$$

From the conditional density function (3.3), the log-likelihood function of a set of observations $\{S_i\}_{i=0}^n$ can be derived:

$$\begin{aligned} \mathcal{L}(a,b,\sigma) &= \sum_{i=1}^{n} \log(f S_i|S_{i-1}; a, b, \sigma) \\ &= -\frac{n}{2}\log(2\pi) - n\log(\hat{\sigma}) - \frac{1}{2\hat{\sigma}^2} \sum_{i=1}^{n} (S_i - S_{i-1}e^{-a\delta} - b(1 - e^{-a\delta}))^2. \end{aligned} \tag{3.4}$$

3.2.2 Maximum likelihood conditions

The maximum of the log-likelihood function (3.4) can be found at the location where all partial derivatives are zero, which leads to the following set of constraints:

$$\begin{aligned}
\frac{\partial \mathcal{L}(a,b,\sigma)}{\partial a} &= 0 \\
&= -\frac{\delta e^{-a\delta}}{\hat{\sigma}^2} \sum_{i=1}^{n} ((S_i - b)(S_{i-1} - b) - e^{-a\delta}(S_{i-1} - b)^2) \\
&\Rightarrow a = \frac{1}{\delta} \log \frac{\sum_{i=1}^{n} (S_i - b)(S_{i-1} - b)}{\sum_{i=1}^{n} (S_{i-1} - b)^2}, \qquad (3.5) \\
\frac{\partial \mathcal{L}(a,b,\sigma)}{\partial b} &= 0 \\
&= \frac{1}{\hat{\sigma}^2} \sum_{i=1}^{n} (S_i - S_{i-1}e^{-a\delta} - b(1 - e^{-a\delta})) \\
&\Rightarrow b = \frac{\sum_{i=1}^{n} (S_i - S_{i-1}e^{-a\delta})}{n(1 - e^{-a\delta})}, \qquad (3.6) \\
\frac{\partial \mathcal{L}(a,b,\sigma)}{\partial \hat{\sigma}} &= 0 \\
&= \frac{n}{\hat{\sigma}} - \frac{1}{\hat{\sigma}^3} \sum_{i=1}^{n} (S_i - b - e^{-a\delta}(S_{i-1} - b))^2 \\
&\Rightarrow \hat{\sigma}^2 = \frac{1}{n} \sum_{i=1}^{n} (S_i - b - e^{-a\delta}(S_{i-1} - b))^2. \qquad (3.7)
\end{aligned}$$

3.2.3 Solution of the conditions

It is observed that conditions (3.5), (3.6) and (3.7) are dependent on each other. However, both a and b are independent of σ, and knowledge of either a or b will directly grant the value of the other. Once a and b are determined, the solution for σ can be found. To solve these equations it is therefore sufficient to find either a or b: This is done by substituting a into condition (3.6).

In order to simplify algebraic manipulations, (3.5) and (3.6) are rewritten using

$$\begin{aligned} S_x &= \sum_{i=1}^{n} S_{i-1}, \\ S_y &= \sum_{i=1}^{n} S_i, \\ S_x x &= \sum_{i=1}^{n} S_{i-1}^2, \\ S_x y &= \sum_{i=1}^{n} S_{i-1} S_i, \\ S_y y &= \sum_{i=1}^{n} S_i^2, \end{aligned}$$

which yields

$$\begin{aligned} a &= \frac{1}{\delta} \log \frac{S_{xy} - bS_x - bS_y + nb^2}{S_{xx} - 2bS_x + nb^2}, \\ b &= \frac{S_y - e^{-a\delta} S_x}{n(1 - e^{-a\delta})}. \end{aligned}$$

Substituting a into b gives

$$nb = \frac{S_y - \left(\frac{S_{xy} - bS_x - bS_y + nb^2}{S_{xx} - 2bS_x + nb^2} \right) S_x}{1 - \left(\frac{S_{xy} - bS_x - bS_y + nb^2}{S_{xx} - 2bS_x + nb^2} \right)},$$

removing denominators, collecting terms, and factoring out b, an explicit solution is found.

3.2.4 The maximum likelihood equations

The final result is the maximum likelihood equations for the, mean

$$b = \frac{S_y S_{xx} - S_x S_{xy}}{n(S_{xx} - S_{xy}) - (S_x^2 - S_x S_y)},$$

mean reversion rate

$$a = -\frac{1}{\delta} \log \frac{S_{xy} - bS_x - bS_y + nb^2}{S_{xx} - 2bS_x + nb^2},$$

and variance

$$\hat{\sigma}^2 = \frac{1}{n}(S_{yy} - 2\alpha S_{xy} + \alpha^2 S_{xx} - 2b(1-\alpha)(S_y - \alpha S_x) + nb^2(1-\alpha^2))$$
$$\Rightarrow \sigma^2 = \hat{\sigma}^2 \frac{2a}{1-\alpha^2},$$

where $\alpha = e^{-a\delta}$.

In Section D.1 in Appendix D, a `MATLAB` implementation of these maximum likelihood equations may be found.

As an example, the Vasicek parameters have been estimated using the 12-month LIBOR rate and are presented in Table 3.2.

Series	a	b	σ
12-M LIBOR	0.1021	0.5913%	0.2321%

Table 3.2: Vasicek model parameters estimated from the 12-M LIBOR rate. The data spans 3 years, from 2 December 2011 to 30 November 2014.

4

Portfolio Simulations

The two portfolio investment strategies that will be focused upon in this chapter are the Constant Proportion Portfolio Insurance (CPPI) and Option Based Portfolio Insurance (OBPI) strategies. Both strategies have already been introduced in Chapter 1, but a quick re-cap of their basic principles will likely not hurt: The CPPI strategy revolves around dynamic rebalancing of the contents portfolio, moving funds between risky and risk-less assets according to a predetermined scheme with an aim of guaranteeing that the portfolio value never drops below a certain threshold; the OBPI strategy, on the other hand, simply entails splitting the available funds between risky assets, risk-less assets and a put option on (part of) the risky assets, in such way that the portfolio value at maturity is guaranteed to be at least equal to some predetermined minimum.

Utilizing the underlying models presented in Chapter 2 with parameters obtained from real-world data through the calibration methods presented in Chapter 3, the portfolio strategies may be numerically simulated an arbitrary number of times for each set of parameters (i.e. for each financial environment that the parameters represent). In this way, the average performances of the different strategies under different financial conditions may be estimated by means of the Monte Carlo method. From these results, the strategies may be compared and conclusions on their performances may be made. The compiled results are be presented in Chapter 5.

For the results to be useful for inter-strategy comparisons, it has in all cases been assumed that the initial portfolio value is equal to one[1]. Furthermore, and for the same reason, it is assumed that the initial proportion of risky assets is equal in either strategy.

The simulations were done in `MATLAB`: The code can be found in Section D.2 in Appendix D.

[1]This may always be done without loss of generality.

4.1 The CPPI strategy

In Section 1.1.1 the CPPI strategy was presented in the context of the continuous Black-Scholes model. It was noted how that particular set-up, paradoxically, implied that if the drift in the underlying was greater than the risk-free interest rate, then the expected return could be increased indefinitely by increasing the multiplier, without any risk of default. In this section it will be shown that in the presence of jumps in the price of the risky asset this is no longer true, and the CPPI strategy may actually fail and breach the floor. Precise analytical conclusions are drawn in Appendix A, even though numerical simulations provide a very illustrative display of this phenomenon.

4.1.1 CPPI in the presence of jumps

As covered in Chapter 2, the dynamics of the risky asset S and the zero-coupon bond B_t may be written as

$$\frac{dS_t}{S_{t-}s} = dZ_t \quad \text{and} \quad \frac{dB_t}{B_{t-}} = dR_t,$$

where Z and R are possibly discontinuous driving processes, modelled as semimartingales. Using the Vasicek model where

$$dr_t = (\alpha - \beta r_t)dt + \sigma dW_t,$$

the zero-coupon is given by

$$B_t = B(t,T) = E[e^{-\int_t^T r_s ds}],$$

from which it follows that

$$\frac{dB_t}{B_t} = r_t dt - \sigma \frac{1 - e^{-\beta(T-t)}}{\beta} dW_t.$$

In the general case, the following assumptions may be made:

(1) $\Delta Z_t > -1$ almost surely.

(2) The zero-coupon price process B is continuous.

The first assumption guarantees positive risky asset prices, while the second allows to focus on the impact on jumps in the underlying asset. In particular, this implies

$$B_t = B_0 \exp\left(R_t - \frac{1}{2}[R]_t\right) > 0 \quad a.s.$$

In reference to Equation (1.1), define $\tau = \inf\{t \,:\, V_t \leq B_t\}$. Since the CPPI strategy is self-financing, up to time τ the portfolio value satisfies

$$dV_t = m(V_{t-} - B_t)\frac{dS_t}{S_t} + \{V_{t-} - m(V_{t-} - B_t)\}\frac{dB_t}{B_t},$$

which may be rewritten in terms of the cushion $C_t = V_t - B_t$ as

$$\frac{dC_t}{C_{t-}} = mdZ_t + (1-m)R_t.$$

By making a *change of numeraire* and introducing the discounted cushion $C_t^* = \frac{C_t}{B_t}$, a simple application of Itô's formula yields

$$\frac{dC_t^*}{C_{t-}^*} = m(dZ_t - d[Z,R]_t - dR_t + d[R]_t). \tag{4.1}$$

Defining

$$L_t \equiv Z_t - [Z,R]_t - R_t + [R]_t, \tag{4.2}$$

Equation (4.1) can be rewritten in a more compact form using the Doléans-Dade exponential $\mathcal{E}$

$$C_t^* = C_t^* \mathcal{E}(mL)_t,$$

where, by definition,

$$\frac{d\mathcal{E}(mL)_t}{\mathcal{E}(mL)_t} = mdL_t.$$

From the definition of the CPPI strategy it follows that after time τ the process C^* remains constant. This means that the discounted cushion value for the strategy can be written explicitly as

$$C_t^* = C_0^* \mathcal{E}(mL)_{t\wedge\tau}, \tag{4.3}$$

or alternatively

$$\frac{V_t}{B_t} = 1 + \left(\frac{V_0}{B_0} - 1\right)\mathcal{E}(mL)_{t\wedge\tau}. \tag{4.4}$$

Since the stochastic exponential can become negative, in the presence of large-enough negative discontinuities in the stock price, Equation (4.4) shows that the capital N is no longer guaranteed at maturity by this strategy.

Formulae for the probability of loss, expected loss and distribution of loss of a portfolio under CPPI-management are derived in Appendix A.

4.1.2 Numerical implementation

The evolution of the CPPI portfolio value follows the SDE

$$\begin{aligned} dV_t &= m(V_{t-} - GB_t)^+ \frac{dS_t}{S_t} + (V_{t-} - m(V_{t-} - GB_t)^+)\frac{dB_t}{B_t} = \\ &= m(V_{t-} - GB_t)^+ dZ_t + (V_{t-} - (V_{t-} - m(V_{t-} - GB_t)^+)\frac{dB_t}{B_t}, \end{aligned}$$

where m is the multiplier, G is the guaranteed amount, and B_t is the price at time t of the zero-coupon bond with nominal one and maturity T (making GB_t equal to the

floor). m is assumed to be dynamic and to depend negatively on the current level of volatility as suggested by Cont and Tankov in 2009 [5]:

$$m_{t_i} = m_0(\frac{\sigma_{t_i}}{\sigma_0})^{0.2}.$$

Discretization of time provides the following algorithm for the portfolio value at dates $t_i \in [0,T]$

$$\begin{aligned} V_{t_i} = \; & V_{t_{i-1}} + m_{t_{i-1}}(V_{t_{i-1}} - GB_{t_{i-1}})^+(Z_{t_i} - Z_{t_{i-1}}) \\ & + (V_{t_{i-1}} - m_{t_{i-1}}(V_{t_{i-1}} - GB_{t_{i-1}})^+)\left(\frac{B_{t_i} - B_{t_{i-1}}}{B_{t_{i-1}}}\right). \end{aligned}$$

4.1.3 Simulation samples

Figure 4.2 shows two trajectories of the CPPI portfolio in a falling and rising market, respectively. In the case of a falling market, it can be clearly seen how the portfolio's exposure to the risky asset is decreased as the portfolio value approaches the floor. This allows it, in this particular case, to avoid default even though the stock plummets far below the floor. In the case of a sustained rise in the market, on the other hand, the portfolio's exposure to the risky asset is instead increased. As a result, the portfolio value follows, to a large extent, the positive development of the stock.

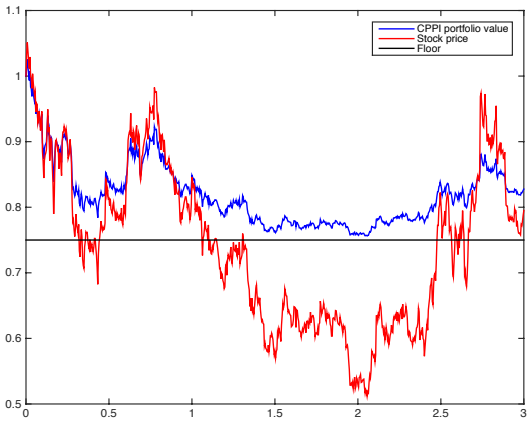

(a) CPPI portfolio value trajectory in a falling market as a function of time (years). Blue line: Portfolio value. Red line: Stock price. Black line: Floor.

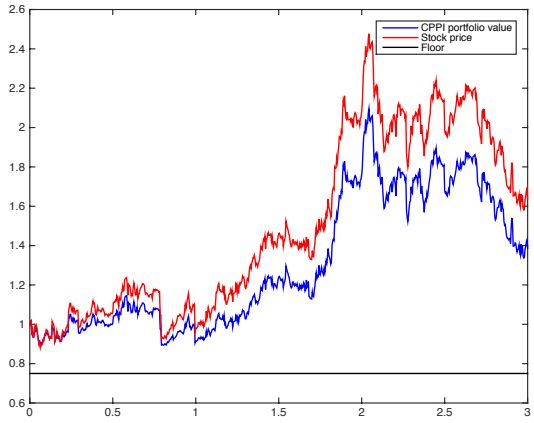

(b) CPPI portfolio value trajectory in a rising market as a function of time (years). Blue line: Portfolio value. Red line: Stock price. Black line: Floor.

Figure 4.1: Trajectories of the CPPI portfolio value in a falling (left) and rising market (right). The floor is equal to 0.75 and the multiplier is equal to 2.5. The parameters used in the simulation model were calibrated using three years of BMW stock price data.

4.2 The OBPI strategy

As has already been described in Section 1.2 and the chapter preamble, the OBPI strategy consists in guaranteeing a certain proportion of the initial portfolio value at maturity, while still being exposed to possible market up-swings, by splitting the available funds between riskless assets, risky assets and a put option on (part of) the risky assets. In contrast to the CPPI strategy, the OBPI strategy can never default: Even if there are jumps in the price of the underlying, or other complicating phenomena for that matter, the definition of the put contract will always guarantee a fixed value at maturity. However, the profitability of the OBPI strategy will, of course, be subject to the dynamics of the put price: For example, it is well-known that the price of the put generally drops very quickly as it approaches maturity, which naturally affects the profitability of the OBPI strategy when implemented on shorter time horizons.

4.2.1 Numerical implementation

Let $(V_t)_{t\in[0,T]}$ denote the value of the OBPI portfolio at time t, S_t the stock price and B_t the price of the zero-coupon bond. Furthermore, let θ_t denote the amount of shares of the risky asset held at time t and $p(\theta_t, K, T-t)$ the price of the European put option for θ_t shares with strike K and time to maturity $T-t$. In the strategy under investigation, the number of shares held at any time does not chance during the lifetime of the strategy, and θ_t may therefore simply be referred to as θ. Since the portfolio is self-financing, the value of the portfolio between two dates t_i and t_{i+1} must change according to

$$V_{t_{i+1}} - V_{t_i} = \theta(S_{t_{i+1}} - S_{t_i}) + (V_{t_i} - \theta S_{t_i})\frac{B_{t_{i+1}} - B_{t_i}}{B_{t_i}} + p(\theta, K, T-t_{i+1}) - p(\theta, K, T-t_i).$$

The values of S_t and B_t are modelled according to the set-up of Chapter 2, and the price of the put is estimated using formula (B.4) derived in Appendix B. Since the definition of the OBPI strategy implies that the allocation of wealth remains unchanged throughout the lifetime of the strategy, it is for most purposes sufficient to estimate the terminal value of the portfolio

$$V_T = V_0 + \theta(S_T - S_0) + (V_0 - \theta S_0)\frac{1 - B_0}{B_0} + (K - \theta S_T)^+ - p(\theta, K, T).$$

Just as in the CPPI case, the initial value V_0 is assumed to be equal to one. The capital not invested in the risky asset is split between the put on the risky asset and the riskless asset.

4.2.2 Simulation samples

Figure 4.2 shows two trajectories of the CPPI portfolio in a falling and rising market, respectively. As the put is used to hedge the portfolio, it can never default. However, before maturity it's value may, under certain circumstances, be below the floor. In upwards markets, obviously, the partial exposure to the risky asset allows the portfolio value to grow. An illustration of the European put dynamics is shown in Figure 4.3.

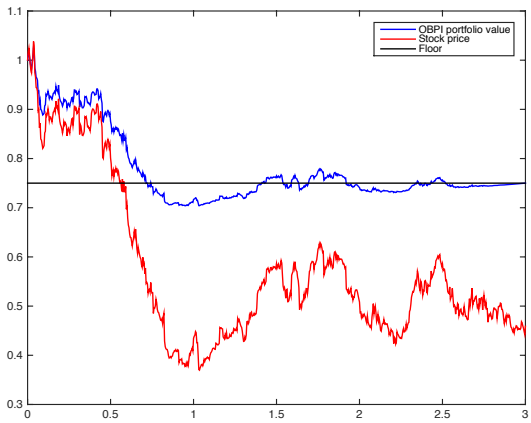

(a) OBPI portfolio value trajectory in a falling market as a function of time (years). Blue line: Portfolio value. Red line: Stock price. Black line: Floor.

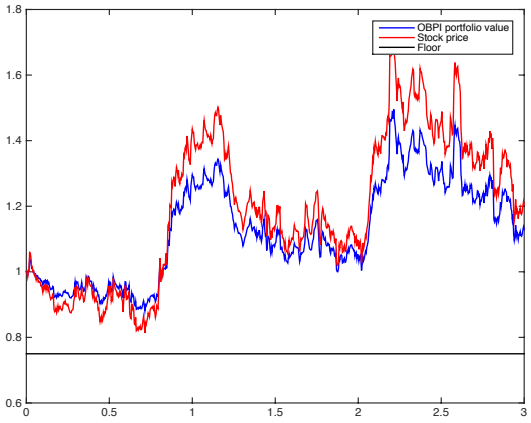

(b) OBPI portfolio value trajectory in a rising market as a function of time (years). Blue line: Portfolio value. Red line: Stock price. Black line: Floor.

Figure 4.2: Trajectories of the OBPI portfolio value in a falling (left) and rising market (right). The floor is equal to 0.75 and initial amount of stocks equals to 0.7342. The parameters used in the simulation model were calibrated using three years of BMW stock price data.

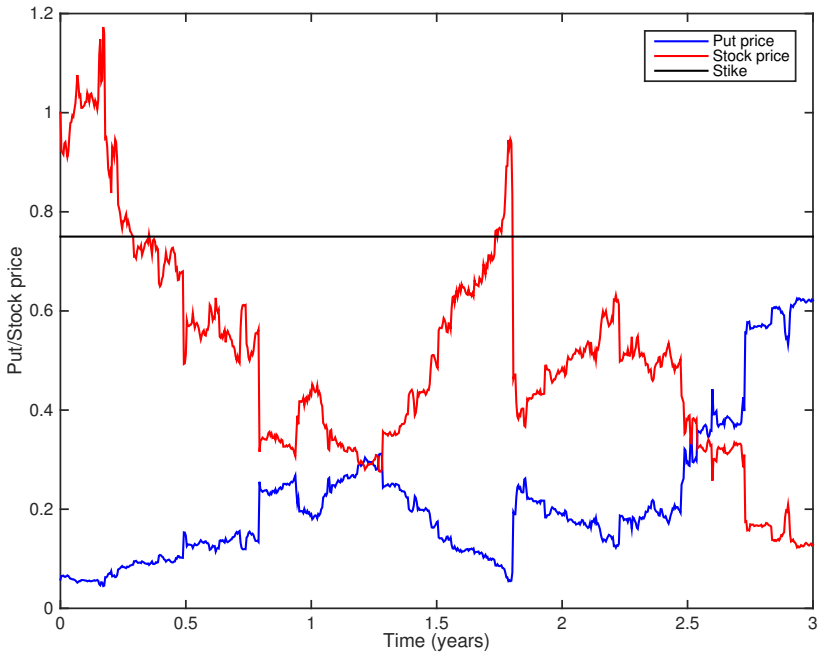

Figure 4.3: Dynamics of the European put option. Blue line: Put price. Red line: Stock price. Black line: Strike.

5

Results

Calibration and simulation has been carried out as described in Chapter 3 and Chapter 4, respectively. The results are presented in this chapter, and discussed and interpreted in Chapter 6. In terms of calibration, focus was set on exploring the properties of the calibration of the Kou model. The properties of the classical maximum likelihood method are therefore not explored in depth. In terms of simulations, the CPPI and OBPI strategies have been simulated and tested under various circumstances. In particular, the dependence on multiplier and time to maturity is looked into. The portfolio performance levels in different market types are also investigated.

5.1 Model calibration results

The parameters of the Kou model were determined through calibration towards real-world financial data of three indices and three stocks. For each index or stock, data corresponding to one, three, and ten years, spanning backwards from November 30 2014, was used in order to find the parameters. Complete calibration results are presented in Table 5.1. Illustrations of the goodness of fit achieved are presented for MSFT stock and SX5E index data in Figure 5.1. Additional goodness of fit results are presented in Appendix C, for the NIKKEI225 and SNP500 indices and BMW and AZN stocks.

The rather straight-forward use of the maximum likelihood method yielded the results found in Table 5.2 and Table 5.3 for the Vasicek model and stochastic volatility, respectively, where the interest rate was calibrated towards the LIBOR rate and stochastic volatility towards stock price volatility.

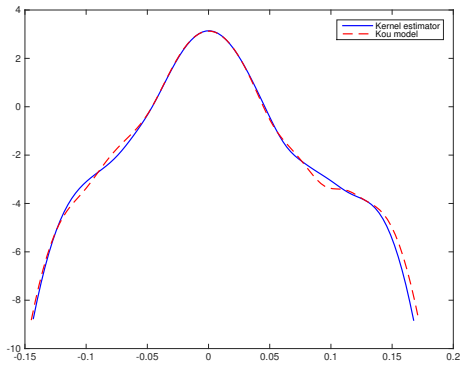

(a) 10 years of MSFT stock data.

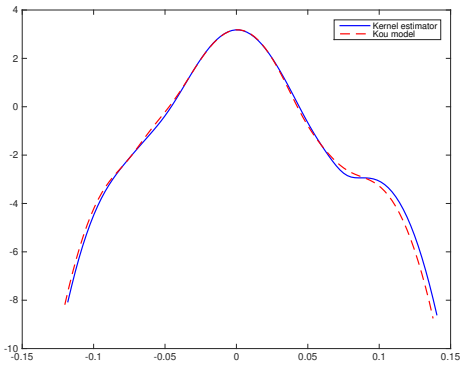

(b) 10 years of SX5E index data.

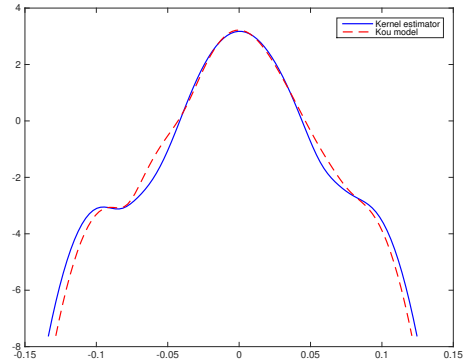

(c) Three years of MSFT stock data.

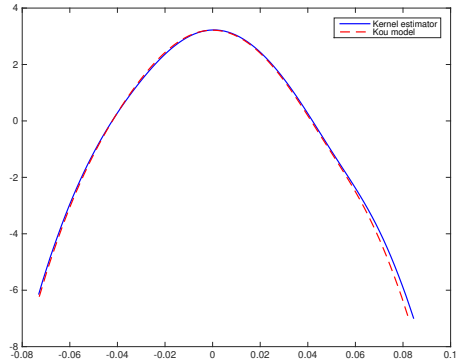

(d) Three years of SX5E index data.

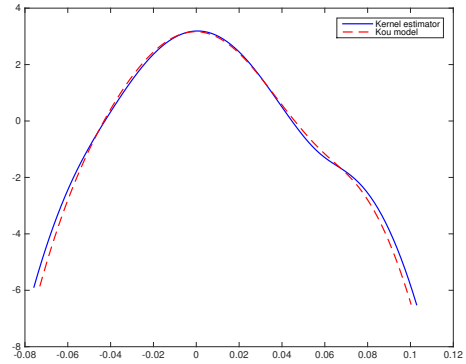

(e) One year of MSFT stock data.

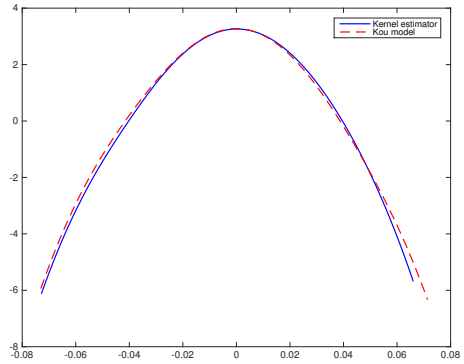

(f) One year of SX5E index data.

Figure 5.1: Logarithm of the densities corresponding to ten, three and one years of MSFT stock and SX5E index time series. Solid lines: Kernel density estimator applied directly on data. Dashed lines: Kou model simulations with parameters estimated via empirical characteristic exponent. All data used spans backwards from 30 November, 2014.

Series	μ	σ	λ	p	η_+	η_-
NIKKEI225 10yr	0.1575	0.1704	33.1174	0.5913	0.0172	0.0175
NIKKEI225 3yr	0.1875	0.1664	94.7402	0.4473	0.0081	0.0091
NIKKEI225 1yr	0.5744	0.1432	182.3641	0.8969	0.0120	0.0043
SNP500 10yr	0.2833	0.1240	50.8535	0.6689	0.0175	0.0154
SNP500 3yr	0.1806	0.0996	116.8213	0.3856	0.0032	0.0053
SNP500 yr	0.7587	0.0770	256.4353	0.7789	0.0018	0.0036
SX5E 10yr	0.5489	0.1360	110.7297	0.7867	0.0170	0.0109
SX5E 3yr	0.4942	0.1477	124.2325	0.8578	0.0104	0.0055
SX5E 1yr	0.0505	0.1198	231.7510	0.4328	0.0037	0.0052
BMW 10yr	0.0472	0.2438	55.7988	0.3991	0.0192	0.0262
BMW 3yr	0.3641	0.1582	374.7105	0.4428	0.0058	0.0086
BMW 1yr	2.6611	0.0721	679.7303	0.9180	0.0107	0.0051
MSFT 10yr	0.2153	0.1707	50.1890	0.6490	0.0217	0.0166
MSFT 3yr	0.1078	0.1129	133.0564	0.4594	0.0109	0.0112
MSFT 1yr	1.9153	0.0720	742.9403	0.8921	0.0104	0.0038
AZN 10yr	0.0480	0.1797	42.0319	0.4514	0.0174	0.0206
AZN 3yr	0.2550	0.1603	7.1010	0.8237	0.0685	0.0296
AZN 1yr	0.3445	0.1794	12.7312	0.6941	0.0664	0.0382

Table 5.1: Kou model parameters estimated from historical data of the NIKKEI225, SNP500 and SX5E indeces, and BMW, MSFT and AZN stocks. As indicated in the table, the historical data used in the calibration spans ten, three and one year backwards from November 30, 2014.

5.2 Portfolio simulation results

By performing very large numbers of simulations[1], the Monte Carlo method was applied to measure the performances of the portfolio strategies. Portfolio performances over a 5-year investment period, for varying CPPI multipliers, are presented in Table 5.4 in the case of an index underlying. The dependence on time to maturity was also investigated, and the results are presented in Table 5.5 in the case of a high-volatility stock underlying.

In Figure 5.2, the dependence of loss probability (from the point of view of the issuer of the portfolio) on the multiplier for a CPPI portfolio containing MSFT, BMW and AZN stocks or SNP500, NIKKEI225, and SX5E indices, is shown.

[1] 100 000 simulations were done to obtain each data point.

Series	a	b	σ
12-M LIBOR	0.1021	0.5913%	0.2321%
6-M LIBOR	0.0912	0.6136%	0.2419%

Table 5.2: Vasicek model parameters estimated from the 12-M and 6-M LIBOR rate. The data spans 3 years, from 2 December 2011 to 30 November 2014.

Series	k	θ	δ
NIKKEI225	3.721	0.1453	0.3376
SNP500	3.221	0.1288	0.2704
SX5E	2.289	0.1012	0.1789
BMW	4.422	0.1843	0.3954
MSFT	4.162	0.1707	0.3678
AZN	3.332	0.1612	0.3419

Table 5.3: Stochastic volatility parameters estimated from historical data of the NIKKEI225, SNP500 and SX5E indeces, and BMW, MSFT and AZN stocks. The data spans 3 years, from 2 December 2011 to 30 November 2014.

The graphs in Figure 5.2 were obtained through the following process:

(1) The multiplier is set equal to a pre-determined initial value for the parameter sweep.

(2) For each stock or index, 100 000 CPPI portfolio trajectories are calculated.

(3) For each trajectory, the final value is compared to the floor.

(4) The proportion of defaulting portfolios is calculated.

(5) The multiplier is increased by a predetermined step length.

(6) Steps (2) to (5) are repeated until the final multiplier value has been covered.

It may be observed, for example from Table 5.4, that in the case of more regular market conditions, the CPPI strategy is generally slightly outperformed by the OBPI strategy, both in terms of returns and portfolio volatility. This results hold true even as the lifetime of the strategy or volatility is varied slightly. However, as may be observed in Table 5.5, the performances in very changing markets, as exemplified by the very volatile MSFT stock, the OBPI performs much worse. Especially on shorter time horizons, the OBPI is outperformed by the CPPI strategy.

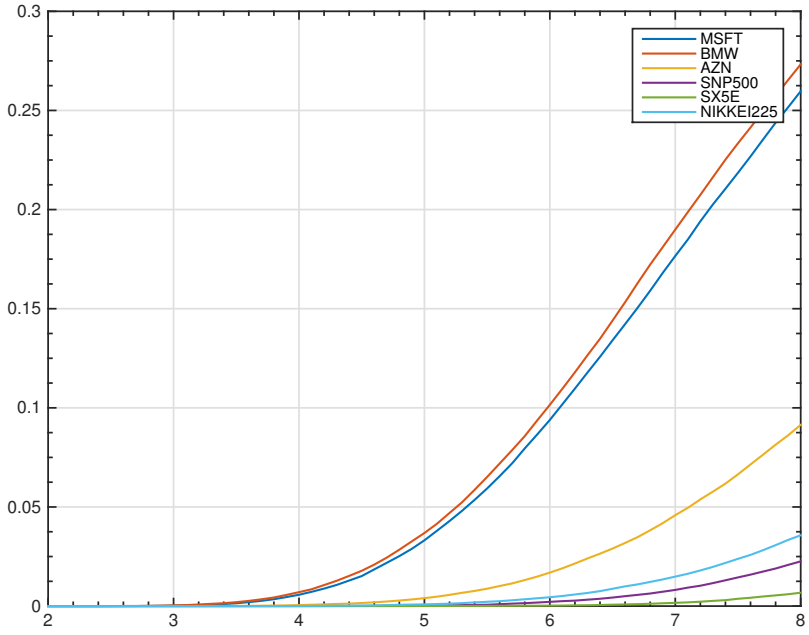

Figure 5.2: Simulated probability of loss as a function of the multiplier for a 5-year investment period.

Multiplier value	2	2.5	3.5	5
CPPI annual return	4.893%	6.121%	8.781%	15.452%
CPPI annual volatility	0.0912	0.1252	0.1524	0.2321
OBPI annual return	4.992%	6.213%	8.911%	16.114%
OBPI annual volatility	0.08991	0.1233	0.1457	0.2231

Table 5.4: Simulated CPPI and OBPI performance over an investment period of 5 years based on NIKKEI225 index, for different multiplier values. The floor of the CPPI portfolio was set to 85%, and the OBPI portfolio had the same initial risky asset investment proportion as the CPPI portfolio.

Time to maturity	1.5 yr	3 yr	5 yr	10 yr
CPPI annual return	6.128%	7.134%	9.589%	13.513%
CPPI annual volatility	0.1244	0.1341	0.1524	0.1922
CPPI default probability	0.623%	1.242%	1.811%	2.512%
OBPI annual return	2.223%	5.234%	8.891%	12.514%
OBPI annual volatility	0.1141	0.1289	0.1461	0.1821

Table 5.5: Simulated CPPI and OBPI performance over various lengths of investment periods based on MSFT stock, with the multiplier set equal to 3.5. The floor of the CPPI portfolio was set to 85%, and the OBPI portfolio had the same initial risky asset investment proportion as the CPPI portfolio.

6

Discussion and Conclusions

In the introduction in Chapter 1, the importance of a proper theoretical framework when analysing portfolio insurance strategies was pointed out. Having this in mind, a model that would reflect the empirical behaviour of asset prices was set up in Chapter 2. Lévy processes were used to model stock price dynamics, while stochastic volatility was implemented to account for volatility clustering phenomena and the Vasicek model was used to describe fluctuations in the bond market. The various models were calibrated using the methods presented in Chapter 3. By means of the Monte Carlo method, results on the performance of the CPPI and OBPI strategies were obtained.

The results of both the calibration and simulations are discussed. Concerning the calibration, the focus of the discussion is on the Kou model and its behaviour. The maximum likelihood method, that was also applied, is extensively covered in the literature. Concerning the simulations, the results are discussed and some explanations are given.

6.1 Concerning calibration

The calibrated parameters of the Kou model show dependence on the length of the time-span over which the data stretches: In the case of shorter time spans, as opposed to longer time spans, the following is generally observed

(1) Volatility, σ, is calibrated to a lower value.

(2) Jump intensity, λ, is calibrated to a higher value.

(3) The probability of negative jumps, p, is calibrated to a higher value.

(4) The sizes of occurring positive and negative jumps, η_+ and η_-, are calibrated to lower values.

One may wonder what's behind these generally observed changes in calibration results? In fact, they may be considered quite natural: As the observed time-span becomes smaller, each intra-day jump becomes more important in relation to the over-all movements of the asset price over the time-span in question. The calibration method will then, in a sloppy sense of speaking, "interpret" a larger part of the intra-day changes as jumps, rather than as part of the process's volatility, thereby yielding a smaller volatility parameter by a larger jump intensity parameter. However, as most intra-day changes are relatively small, the characteristic lengths of the jumps are decreased. It turns out the it is negative, to a larger extent than positive, intra-day movements that are now interpreted as jumps, and therefore the probability of negative jumps is calibrated higher, while the characteristic length of negative jumps is decreased to a larger extent than that of positive jumps.

6.2 Concerning simulation

Figure 5.2 shows the dependence of the simulated loss probability (from the point of view of the issuer of the portfolio) on the multiplier for a CPPI portfolio containing MSFT, BMW and AZN stocks or SNP500, NIKKEI225, and SX5E indices. The loss probabilities for MSFT and BMW are quite similar, exhibiting 5% loss probabilities at multiplier values of about 5.5. AZN is significantly less risky: only at a multiplier value of 7 does the stock reach a 5% probability of loss. Portfolios written on the indices behave quite similarly to each other as far as probability of loss is concerned, with significant loss probabilities only for very high multipliers.

The probability of breaching the floor of a CPPI managed portfolio is given by Equation (A.1). In the case when the (discounted) risky asset price process follows the Kou model, this means

$$P[\exists t \in [0,T] : V_t \leq B_t] = 1 - \exp(-Tp\lambda(1 - 1/m)^{\eta_-}). \tag{6.1}$$

The obtained results of Figure 5.2 coincide very well with the graphs predicted by Equation (6.1). This is a satisfactory result from a stimulatory point of view, as it supports that the model has been correctly implemented.

Since, in the case of a less erratic underlying, the CPPI only has a negligible risk of breaching the floor, it is a very good alternative to the OBPI portfolio when the options market is not liquid. Under these conditions, CPPI is only slightly outperformed by the OBPI strategy.

However, when the market is very volatile OBPI performs poorly. This is especially true with shorter times to maturity, as the put option loses much of its value in the last months before maturity, while it may still be quite expensive to by at initiation due to the high market volatility. On the other hand, under these conditions the CPPI strategy has a non-negligible risk of default. This risk, naturally, grows with the length of the time-horizon over which the strategy is applied. It may further be observed that the higher the volatility, the more does the CPPI outperform the OBPI portfolio, whereas

higher intensity or sizes of jumps favours the OBPI strategy. Furthermore, the difference between the two portfolios decreases as the floor increases.

6.3 Further research

With only one year of data, the calibrations start to sway slightly as the starting point for the search algorithm is altered. More research could go into investigating how the stability of the short-span calibrations can be improved, and how their stability can best be quantified. Furthermore, more advanced methods can be used to calibrate and incorporate the stochastic volatility together with the Kou model. This is actually a rather vast subject to look into, and could well be the topic of future master's theses.

On the simulation side, if would be interesting to look into the behaviour of the investment strategies under more specific market conditions, such as purely falling or rising markets. It would also be interesting to look at more advanced portfolio insurance strategies where, for example, the guaranteed amount can be more complex and depend on the trajectory taken by the portfolio. An example, taken from the real world, of this is when the value at maturity is guaranteed to be equal to the maximum of a pre-determined floor and a certain percentage of the maximum portfolio value attained during the lifetime of the portfolio: E.g. at maturity the portfolio pay-off is equal to the maximum of 90% of the initial value and 70 % of the maximum portfolio value achieved during the life of the portfolio. Furthermore, research into the pricing of so-called *crash bonds* could provide useful insights into the possibilities to protect the CPPI portfolio from default.

Bibliography

[1] P Bertrand and J. Prigent. Portfolio Insurance Strategies: A Comparison of Standard Methods When the Volatility of the Stock is Stochastic. *International Journal of Business*, 8(4):15–31, 2003. ISSN 1083-4346. doi: 10.2139/ssrn.450061. URL `http://dx.doi.org/10.2139/ssrn.450061`.

[2] D Bisias, M. Flood, A.W Lo, and S. Valavanis. A Survey of Systemic Risk Analytics. *Annual Review of Financial Economics*, 4(1):255–296, October 2012. ISSN 1941-1367. doi: 10.1146/annurev-financial-110311-101754. URL `http://hdl.handle.net/1721.1/87772`.

[3] F. Black and R. Jones. Simplifying portfolio insurance. *The Journal of Portfolio Management*, 14(1):48–51, 1987. doi: 10.3905/jpm.1987.409131. URL `http://dx.doi.org/10.3905/jpm.1987.409131`.

[4] Y. Bu. Option Pricing Using Lévy Processes. *Master's thesis*, 2007. URL `http://www.math.chalmers.se/~palbin/YongqiangBu.pdf`.

[5] Rama Cont and Peter Tankov. Constant Proportion Portfolio Insurance in presence of Jumps in Asset Prices. *Mathematical Finance*, 19(3):379–401, July 2009. ISSN 0960-1627. doi: 10.1111/j.1467-9965.2009.00377.x. URL `http://onlinelibrary.wiley.com/doi/10.1111/j.1467-9965.2009.00377.x/abstract`.

[6] N. El Karoui, M. Jeanblanc, and V. Lacoste. Optimal portfolio management with American capital guarantee. *Journal of Economic Dynamics and Control*, 29(3):449–468, March 2005. ISSN 0165-1889. doi: doi:10.1016/j.jedc.2003.11.005. URL `http://www.sciencedirect.com/science/article/pii/S0165188904000442`.

[7] Ken iti Sato. *Lévy Processes and Infinitely Divisible Distributions*, volume 68 of *Cambridge Studies in Advanced Mathematics*. Cambridge University Press, Cambridge, November 1999. ISBN 9780521553025.

[8] Niels Jacob and René L. Schilling. An analytic proof of the Lévy–Khinchin formula on R^n. *Publ. Math. Debrecen*, 53(1-2):69–89, 1998. ISSN 2064-2849

(Online). URL http://www.math.tu-dresden.de/sto/schilling/sources/pa/schilling10.pdf.

[9] Fima C. Klebaner. *Introduction to Stochastic Calculus With Applications*. Imperial College Press, London, 3rd edition, March 2012. ISBN 9781848168329.

[10] Steven G. Kou. A jump-diffusion model for option pricing. *Management Science*, 48(8):1086–1101, August 2002. ISSN 1526-5501. doi: 10.1287/mnsc.48.8.1086.166. URL http://dx.doi.org/10.1287/mnsc.48.8.1086.166.

[11] H.E. Leland and M. Rubinstein. The Evolution of Portfolio Insurance. *Portfolio Insurance: A guide to Dynamic Hedging, DL Luskin (ed.)*, pages 3–10, August 1986.

[12] André Perold. Constant Proportion Portfolio Insurance. *Unpublished manuscript*, August 1986. URL http://www.hbs.edu/faculty/Pages/item.aspx?num=4800.

[13] Philip E. Protter. *Stochastic Integration and Differential Equations*, volume 21 of *Stochastic Modelling and Applied Probability*. Springer, Berlin, 2nd edition, 2005. ISBN 9783662100615.

[14] C. Rama and E. Voltchkova. Integro-differential equations for option prices in exponential Lévy models. *Finance and Stochastics*, 9(3):299–325, July 2005. ISSN 1432-1122 (Online). doi: 10.1007/s00780-005-0153-z. URL http://link.springer.com/article/10.1007%2Fs00780-005-0153-z.

[15] M Tisserand. Exponential of Lévy processes as a stock price - Arbitrage opportunities, completeness and derivatives valuation. *Master's thesis*, 2006. URL http://edoc.hu-berlin.de/master/tisserand-marc-2006-07-25/PDF/tisserand.pdf.

[16] Jun Yu. Empirical Characteristic Function Estimation and Its Applications. *Economic Reviews*, 23(2):93–123, May 2004. ISSN 1532-4168 (Online). doi: 10.1081/ETC-120039605. URL http://ideas.repec.org/a/taf/emetrv/v23y2004i2p93-123.html.

A

More on CPPI in the presence of jumps

Stochastic calculus provides the required tools for deeper analysis of the CPPI portfolio strategy, when the risky asset is modelled as the solution to a jump-diffusion type stochastic differential equation. The analysis of Section 4.1.1 demonstrates that in the presence of jumps in the risky asset, there is a non-zero risk of default to the CPPI portfolio. This section elaborates on this matter by finding formulae for the probability of default, expected loss-size, and distribution of losses. From the point of view of a professional (or amateur for that matter) portfolio manager, this is fundamental in judging and sizing the risks that the portfolio under management is subjected to at any point in time.

A.1 Probability of loss

A CPPI portfolio incurs a loss (breaks through the floor) if, for some $T \in [0,T]$, $V_t \leq B_t$. The event $V_t \leq B_t$ is equivalent to $C_t^* \leq 0$ and since R is continuous and $\mathcal{E}(X)_t = \mathcal{E}(X)_{t-}(1 + \Delta X_t)$, $C_t^* \leq 0$ for some $T \in [0,T]$ if and only if $m\Delta L_t \leq -1$ for some $T \in [0,T]$, as follows from Equation (4.3). This leads to the following result [5, p. 384].

Proposition A.1. *Let L be of the from $L = L^c + L^j$, where L^c is a continuous process and L^j is an independent Lévy process with Lévy measure ν. Then the probability of going below the floor is given by*

$$P[\exists t \in [0,T] : V_t \leq B_t] = 1 - \exp\left(-T \int_{-\infty}^{-1/m} \nu(dx)\right). \tag{A.1}$$

Proof. This result follows from the fact that the number of jumps of the Lévy process L^j in the interval $[0,T]$ whose sizes fall in $(-\infty, -1/m]$ is a Poisson random variable with

intensity $T\nu((-\infty, -1/m])$. □

Corollary A.1. *Assume that S follows an exponential Lévy model of the form*

$$S_t = S_0 e^{N_t},$$

where N is a Lévy process with Lévy measure ν. Then the probability of going below floor is given by

$$P[\exists t \in [0,T] : V_t \leq B_t] = 1 - \exp\left(-T \int_{-\infty}^{\log(1-1/m)} \nu(dx)\right). \tag{A.2}$$

Proof. If follows from Proposition A.1 that there exists another Lévy processes L satisfying

$$\frac{dS_t}{S_t-} = dL_t.$$

The Lévy measure of L is given by

$$\tilde{\nu}^L(A) = \int 1_A(e^x - 1)\nu(dx).$$

Applying Proposition A.1 concludes the proof. □

A.2 Expected loss

With an aim of calculating the expectation of loss, and possibly various other functionals (risk measures), a closer look is taken at the distribution of loss of a CCPI-managed portfolio given that a loss occurs.

In order to obtain explicit formulae, it is assumed that the process L appearing in the stochastic exponential in Equation (4.4) is a Lévy process, whose Lévy measure is denoted ν. It is always possible to write $L = L^1 + L^2$ where L^2 is a process with piecewise constant trajectories and jumps satisfying $\Delta L^2_t \leq -1/m$ and L^1 is a process with jumps satisfying $\Delta L^1_t > -1/m$. In other word, L^1 has Lévy measure $\nu(dx)1_{x>-1/m}$ and L^2 has Lévy measure $\nu(dx)1_{x\leq -1/m}$, no diffusion component, and no drift. Denote by $\lambda^* := \nu((-\infty, -1/m])$ the jump intensity of L^2, by τ the time of occurrence of the first jump of L^2 (it is an exponential random variable with intensity λ^*), and by $\tilde{L}^2 = \Delta L^2_t$ the size of the first jump of L^2. Let the characteristic function of the Lévy process $\log \mathcal{E}(mL^1)_t$ be denoted by ϕ_t and define $\psi(u) = \frac{1}{t}\log \phi_t(u)$. Finally, the assumption $C^*_0 = 1$ may be made without loss of generality.

Now, the expectation of loss may be calculated [5, p. 385].

Proposition A.1. *Assume*

$$\int_1^\infty x\nu(dx) < \infty.$$

Then the expectation of loss conditional on that a loss occurs is

$$E[C_T^*|\tau \leq T] = \frac{\lambda^* + m\int_{-1}^{-1/m} x\nu(dx)}{(1-e^{-\lambda^* T})(\psi(-i)-\lambda^*)}(e^{-\lambda^* T}\phi_T(-i)-1),$$

and the unconditional loss satisfies

$$E[C_T^* 1_{\tau\leq T}] = \frac{\lambda^* + m\int_{-1}^{-1/m} x\nu(dx)}{\psi(-i)-\lambda^*}(e^{-\lambda^* T}\phi_T(-i)-1), \tag{A.3}$$

Proof. The discounted cushion satisfies

$$C_T^* = \mathcal{E}(mL^1)_{\tau\wedge T}\,(1+m\tilde{L}^2 1_{\tau\leq T}) = \mathcal{E}(mL^1)_T\,1_{\tau>T} + \mathcal{E}(mL^1)_\tau\,(1+m\tilde{L}^2)1_{\tau\leq T}. \tag{A.4}$$

Since L^1 and L^2 are Lévy processes, τ, $\tilde{L}^2$ and L^1 are independent. From [7, Theorem 25.17 on p. 319] and the definition of ϕ_t,

$$E[\mathcal{E}(mL^1)_t] = \phi_t(-i),$$

and therefore

$$\begin{aligned} E[C_T^*|\tau\leq T] &= \frac{E[1+m\tilde{L}^2]}{1-e^{-\lambda^* T}}\int_0^T \lambda^* e^{-\lambda^* t}E[\mathcal{E}(mL^1)_t]dt \\ &= \left(\lambda^* + m\int_{-1}^{-1/m} x\nu(dx)\right)\frac{1}{1-e^{-\lambda^* T}}\int_0^T e^{-\lambda^* t}\phi_t(-i)dt, \end{aligned}$$

from which the result follows. □

Remark A.1. Denote by (σ^2,ν,γ) the characteristic triplet of L with respect to zero truncation function (general Lévy processes may be treated similarly by applying a somewhat heavier notation) and suppose that $\int_{\mathbb{R}}|x|\nu(dx)<\infty$. By [5, Proposition A.1 on p. 399] and the Lévy-Khintchine representation [see 8], the characteristic exponent of $\log\mathcal{E}(mL)_t$ is given by

$$\begin{aligned} \psi(u) &= -\frac{m^2\sigma^2u^2}{2} + iu\left(m\gamma - \frac{\sigma^2m^2}{2}\right) + \int_{z>-1/m}(e^{iu\log(1+mz)}-1)\nu(dz) \qquad \text{(A.5)} \\ \psi(-i) &= m\gamma + m\int_{z>-1/m} z\nu(dz). \end{aligned}$$

From Equation (A.4) is follows that the expected gain conditional on that the floor is not broken satisfies

$$E[C_T^*|\tau>T] = E[\mathcal{E}(mL^1)_T] = \phi_T(-i) = \exp\left\{Tm\gamma + Tm\int_{z>-1/m} z\nu(dz)\right\}.$$

Therefore, similarly to the Black-Scholes case covered in Section 1.1.1, conditional expected gain in an exponential Lévy model is increasing with the multiplier, provided the underlying Lévy process has a positive expected return.

A.3 Loss distribution

In order to calculate various risk measures, the distribution function of the loss given that a loss occurs is needed. That is, the quantity

$$P[C_T* < x|\tau \leq T]$$

for $x < 0$. One approach for calculating this conditional distribution function, which will be studied here in what follows, is to express its characteristic function explicitly in terms of the characteristic exponents of the Lévy processes involved and then recover the distribution function by means of numerical Fourier inversion [5, pp. 386–387].

In the following theorem,

$$\tilde{\phi} := \frac{1}{\lambda^*} \int_{-\infty}^{-1/m} e^{iu \log(-1-mx)} \nu(dx)$$

denotes the characteristic function of $\log(-1 - m\tilde{L}^2)$.

Theorem A.1. *Consider a random variable X^* with characteristic function $\phi*$, such that $E[|X^*|] < \infty$ and $\dfrac{|\phi^*(u)|}{1+|u|} \in L^1$. If*

$$\frac{|\tilde{\phi}(u)|}{(1+|u|)|\lambda^* - \psi(u)|} \in L^1$$
$$\int_{\mathbb{R}\setminus[-\epsilon,\epsilon]} |\log|1+mx||\nu(dx) < \infty \tag{A.6}$$

for sufficiently small ϵ, then for every $x < 0$,

$$P[C_T^* < x|\tau \leq T] = P[-e^{X^*} < x] + \frac{1}{2\pi} \int_{\mathbb{R}} e^{-iu\log(-x)} \left(\frac{\lambda^* \tilde{\phi}(u)}{iu(\lambda^* - \psi(u))} \frac{1 - e^{-\lambda^* T + \psi(u)T}}{1 - e^{-\lambda^* T}} - \frac{\phi^*(u)}{iu} \right) du. \tag{A.7}$$

Remark A.1. The random variable X^* is needed only for the purpose of Fourier inversion: the cumulative distribution function of the loss distribution is not integrable and its Fourier transform cannot be computed, but the difference of two distribution functions has a well-defined Fourier transform. In practice, X^* can always be taken equal to a standard normal random variable [5, p. 387].

Proof. It follows from Equation (A.4) that the characteristic function of $\log(-C_T^*)$ conditionally on that a loss occurs, satisfies

$$\begin{aligned} E[e^{iu\log(-C_T^*)|\tau \leq T}] &= \frac{1}{1-e^{-\lambda^* T}} \int_0^T \lambda^* e^{-\lambda^* t} E[e^{iu\log(-\mathcal{E}(mL^1)_t(1+m\tilde{L}^2))}] dt \\ &= \frac{1}{1-e^{-\lambda^* T}} \int_0^T \lambda^* e^{-\lambda^* t} e^{t\psi(u)} \tilde{\phi}(u) dt \\ &= \frac{\tilde{\phi}(u)(1 - e^{-\lambda^* T + \psi(u)T})}{(\lambda^* - \psi(u))(1 - e^{-\lambda^* T})}. \end{aligned}$$

The integral in Equation (A.7) converges as $u \to \infty$ due to the theorem's conditions and the fact that

$$\left| \frac{1 - e^{-\lambda^* T + \psi(u)T}}{1 - e^{-\lambda^* T}} \right| < \frac{1 + e^{-\lambda^* T}}{1 - e^{-\lambda^* T}}.$$

Moreover, condition (A.1) is equivalent to

$$E[|\log(-1 - m\tilde{L}^2)|] < \infty$$
$$E[|\log \mathcal{E}(mL^1)_T|] < \infty,$$

which together with the assumption $E[|X^*|] < \infty$ proves that $\phi(u) = 1 + \mathcal{O}(u)$, $\tilde{\phi}(u) = 1 + \mathcal{O}(u)$ and $\phi^*(u) = 1 + \mathcal{O}(u)$ as $u \to 0$, and therefore the integrand in Equation (A.7) is bounded and therefore integrable in the neighbourhood of zero. The proof is completed by applying [5, Lemma B.1 on pp. 399–400]. □

B

Pricing of the European put option with Lévy-exponential underlying process

With an aim of enabling modelling of the OBPI portfolio in the context of a risky asset that follows an exponential Lévy dynamic, the price of the European put option subject to such underlying dynamics needs to be estimated.

In the following calculations the volatility of the underlying is assumed to be constant and equal to σ. The price of the risky asset at time t is denoted by S_t. In this notation, the pay-off function of a European put option with maturity T and strike K is $G(S_T) = (K - S_T)^+$. The following proposition may then be formulated [14]

Proposition B.1. *If $g(x) = G(e^x)$ denotes the log pay-off function on a European option and there exists $R \neq 0$ such that*

(1) $g(x)e^{-Rx}$ has finite variation on $\mathbb{R}$,

(2) $g(x)e^{-Rx} \in L^1(\mathbb{R})$,

(3) $E[e^{RZ_{T-t}}] < \infty$ and $\int_{\mathbb{R}} \frac{|\Phi_{T-t}(u - iR)|}{1 + |u|} du < \infty$,

where Z is the exponential Lévy process and Φ is its characteristic function, then the price at time t of the European put option satisfies

$$P(t,S_t) = \frac{e^{-r(T-t)}}{2\pi} \int_{\mathbb{R}} \hat{g}(u + iR)\Phi_{T-t}(-u - iR)(S_t^0)^{R-iu} du, \tag{B.1}$$

where $\hat{g}(u) = \int_{\mathbb{R}} e^{iux} g(x)dx$, $S_t^0 = e^{r(T-t)}S_t$, and r is the, assumed constant, interest rate.

One may immediately note that the log payoff function under consideration, $g(x) = (K - e^x)$, satisfies the conditions (1) and (2) for any value of $R \in \mathbb{R}$. Furthermore, if the assumption $R < 0$ is made, the following is obtained

$$\begin{aligned}\hat{g}(u+iR) &= \int_{\mathbb{R}} e^{ix(u+iR)}(K-e^x)^+ dx = \int_{-\infty}^{\log(K)} e^{ix(u+iR)}(K-e^x)dx \\ &= \frac{K^{1+iu-R}}{(iu-R)(iu+1-R)} = \frac{e^{\log(K)(1+iu-R)}}{(iu-R)(iu+1-R)}.\end{aligned} \tag{B.2}$$

Moreover, one may write

$$\begin{aligned}(S_t^0)^{R-iu} &= S_t^{R-iu} e^{r(T-t)(R-iu)} = S_t e^{r(T-t)} e^{-r(T-t)(iu+1-R)} S_t^{-(1+iu-R)} \\ &= S_t e^{r(T-t)} \exp(-\log(S_t) - r(T-t)(1+iu-R)).\end{aligned} \tag{B.3}$$

By substituting the results of Equations (B.2) and (B.3) into the option price formula (B.1), the following is obtained

$$\begin{aligned}P(t,S_t) &= \frac{S_t}{2\pi}\int_{\mathbb{R}} e^{(\log(k/S_t)-r(T-t))(iu+1-R)} \frac{\Phi_{T-t}(-u-iR)}{(R-iu)(R-1-iu)} du \\ &= S_t e^{k^f(1-R)} \frac{1}{2\pi}\int_{\mathbb{R}} e^{iuk^f}\Psi(u)du,\end{aligned} \tag{B.4}$$

where $\Psi(u) := \dfrac{\Phi_{T-t}(-u-iR)}{(R-iu)(R-1-iu)}$ and $k^f = \log(K/S_t) - r(T-t)$ is the log-forward moneyness.

At this point, all that remains to do is to find an explicit expression for the characteristic function $\Phi_t(u)$. The type of underlying dynamic under consideration is one of the form $Z_t = \mu t + \sigma W_t + X_t$, where $X_t = \sum_{i=1}^{N} Y_i$ is a compound Poisson process. Therefore, the following proposition may be utilized:

Proposition B.1. *Suppose X is a compound Poisson process with jump intensity λ and jump size distribution $n\nu_0$, then its characteristic function is*

$$E[e^{iuX_t}] = \exp(t\lambda \int_{\mathbb{R}} (e^{iux} - 1)\nu_0(dx)) \tag{B.5}$$

As ν_0 is absolutely continuous with respect to the Lebesque measure with density $\nu_0(dx) = (p\eta_+ e^{-\eta_+ x}\mathbf{1}_{x>0} + (1-p)\eta_- e^{-\eta_-|x|}\mathbf{1}_{x<0})dx$, it is possible to compute $\Phi_t(u)$ as

$$\begin{aligned}\Phi_t(u) = E[e^{iuZ_t}] &= E[e^{iu(\mu t + \sigma w_t + \sum_{i=1}^{N_t} Y_i)}] = \exp(iu\mu t - \frac{1}{2}\sigma^2 u^2 t + t\lambda \int_{\mathbb{R}} (e^{iux}-1)\nu_0(dx)) \\ &= \exp\left(iu\mu t - \frac{1}{2}\sigma^2 u^2 t + t\lambda(\frac{p\eta_+}{\eta_+ - iu} + \frac{(1-p)\eta_-}{\eta_- + iu} - 1)\right).\end{aligned}$$

If, in particular, $\eta_+ < \eta_-$ then $R = \frac{\eta_+ - \eta_-}{2} < 0$ may be chosen. With this R it is easily seen that the second part of condition (3) of Proposition B.1 is fulfilled. It therefore only remains to verify the first part of the condition (3), which is the integrability of $E[e^R Z_{T-t}]$:

$$E[e^R Z_{T-t}] = E[e^{R\mu t + R\sigma W_t + \sum_{i=1}^{N_t} RY_i}] = e^{\mu R t} E[e^{\sigma R\sqrt{t} N(0,1)}] E[e^{\sum_{i=1}^{N_t} RY_i}].$$

As the first two terms are clearly bounded, only the last term needs to be further investigated:

$$\begin{aligned} E[e^{\sum_{i=1}^{N_t} RY_i}] &= E[\sum_{n\in\mathbb{N}} \mathbf{1}_{N_t=n} e^{\sum_{i=1}^{N_t} RY_i}] = \sum_{n\in\mathbb{N}} E[\mathbf{1}_{N_t=n} e^{\sum_{i=1}^{N_t} RY_i}] \\ &= \sum_{n\in\mathbb{N}} P(N_t = n)(E[e^{RY_1}])^n < +\infty, \end{aligned}$$

where the last inequality holds because N_t is a Poisson random variable and $E[e^{RY_1}] < +\infty$.

C

Goodness of fit of the Kou model calibration

Goodness of fit is illustrated through plots of the densities of the data over plots of the densities of simulation results obtained from the models, using the calibrated parameters. The time series for which goodness of fit is illustrated are: NIKKEI225 index, SNP500 index, BMW stocks, and AZN stocks, each over ten, three and one years spanning backwards from November 30, 2014. The graphs corresponding to the indices and stocks may be found in Figure C.1 and Figure C.2, respectively.

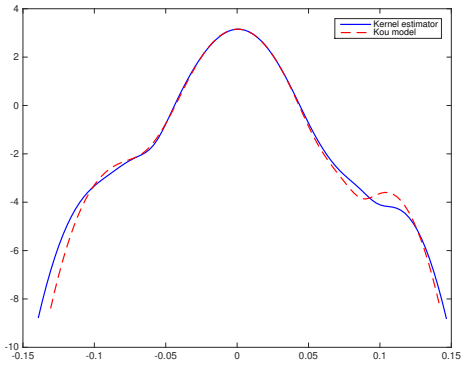

(a) 10 years of NIKKEI225 index data.

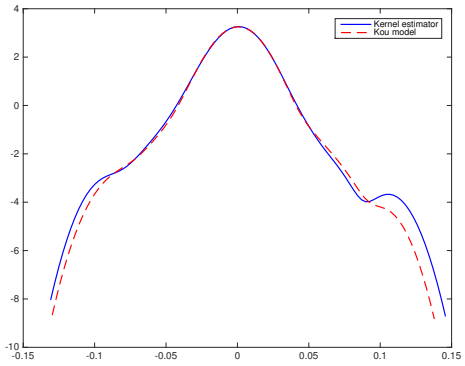

(b) 10 years of SNP500 index data.

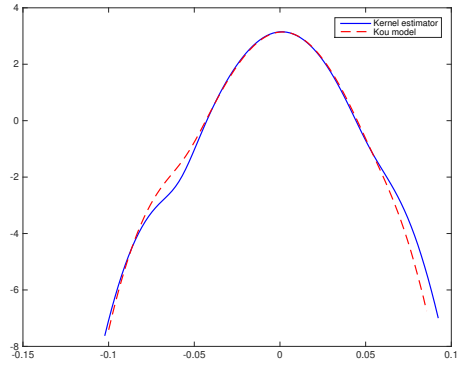

(c) Three years of NIKKEI225 index data.

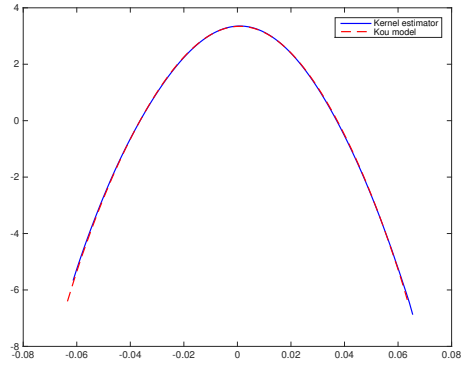

(d) Three years of SNP500 index data.

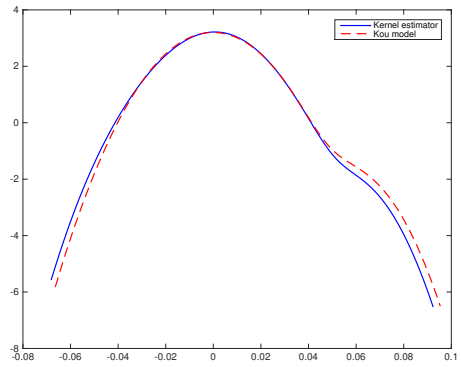

(e) One year of NIKKEI225 index data.

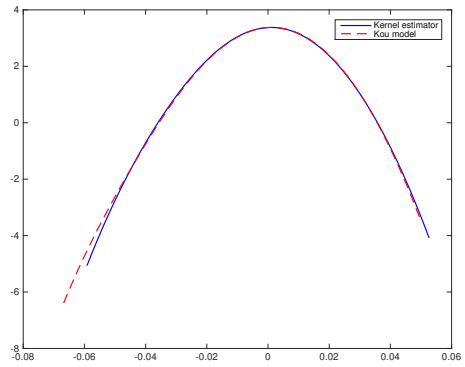

(f) One year of SNP500 index data.

Figure C.1: Logarithm of the densities corresponding to ten, three and one years of NIKKEI225 and SNP500 index time series. Solid lines: Kernel density estimator applied directly on data. Dashed lines: Kou model simulations with parameters estimated via empirical characteristic exponent. All data used spans backwards from 30 November, 2014.

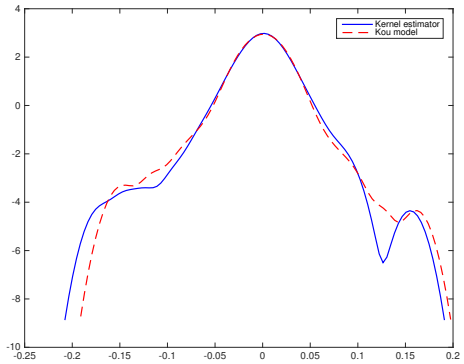

(a) 10 years of BMW stock data.

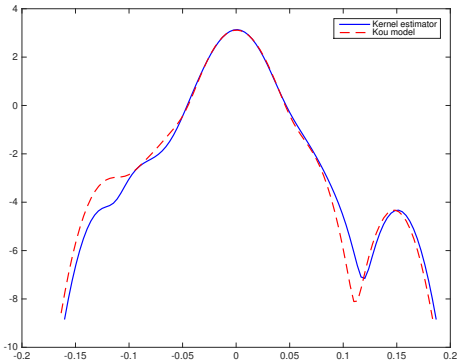

(b) 10 years of AZN stock data.

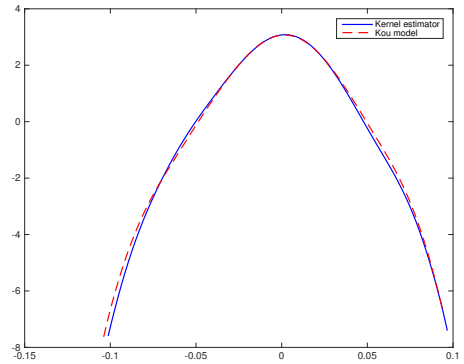

(c) Three years of BMW stock data.

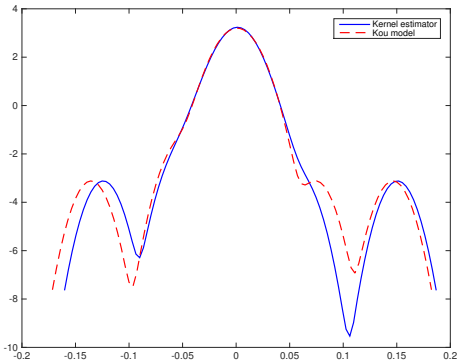

(d) Three years of AZN stock data.

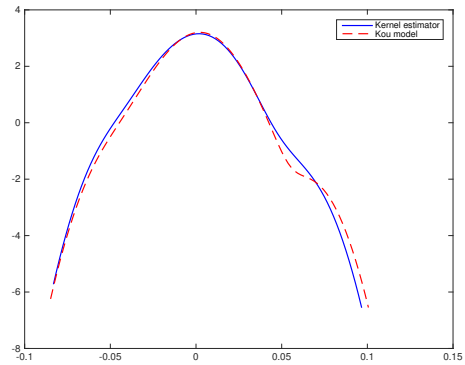

(e) One year of BMW stock data.

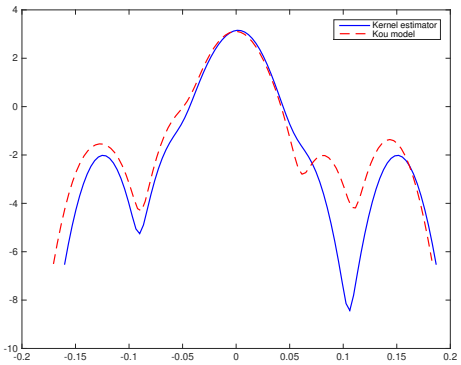

(f) One year of AZN stock data.

Figure C.2: Logarithm of the densities corresponding to ten, three and one years of BMW and AZN stock time series. Solid lines: Kernel density estimator applied directly on data. Dashed lines: Kou model simulations with parameters estimated via empirical characteristic exponent. All data used spans backwards from 30 November, 2014.

D

MATLAB code

Numerical implementations of both calibration and simulation were done in the technical computing language MATLAB. Minor variations to the code were made during it's use, to cover different special cases or parameter inputs. The output of the calibration code was manually inserted into the simulation code. The first line of each file is a comment containing the file name used.

D.1 Calibration code

The code used in calibrating the models is the following:

```
% FILE: parameter_estmation.m

clear
clc

%% Initial guess, parameters and data are defined

% NOTE: mu = theta(1); sigma = theta(2); lambda = theta(3); p =
    theta(4);
% etaPlus = theta(5); etaMinus = theta(6);

disp('The initial guess for the parameter vecor is ([mu sigma
    lambda p etaPlus etaMinus])');
theta0 = [0.25 0.2 50 0.5 0.05 0.05] % Inital guess for theta
K = 60; % +/- K is the upper/lower integration bound, as by
    Cont & Tankov
gap_halfwidth = 0.02; % Half-width of gap around 0 in the
    integration interval
```

```
15
16 stock_prices = csvread('Data/AZN/AZN.csv',2267,0); % csvread
       indices start at 0
17 period_length = round(length(stock_prices)/252); % No. of years
       over which the data stretches
18 time_resolution = period_length/length(stock_prices); % Average
       no. of trading days per year in the data
19
20 % The log returns, i.e. the X_k:s, are calculated
21 log_returns = zeros(length(stock_prices)-1,1);
22 for i=1:(length(stock_prices)-1)
23     log_returns(i) = log(stock_prices(i+1,1)/stock_prices(i,1))
           ;
24 end
25 sigma_star = std(log_returns); % Standard deviation of the log
       returns
26
27 %% The distance integral is defined as a function of theta
28 integrand = @(u, theta) abs(characteristic_exponent(u,theta)
       ...
29     - empirical_characteristic_exponent(u,log_returns,
           time_resolution)).^2 ...
30     .*weight(u,sigma_star);
31 distance = @(theta) integral(@(u) integrand(u, theta),-K, -
       gap_halfwidth) ...
32     + integral(@(u) integrand(u, theta), gap_halfwidth, K);
33
34 %% An optimization routine is used to find the minimizing theta
35 options = optimset('MaxFunEvals', 100000, 'MaxIter',100000, '
       TolX', 1e-6);
36 lb=[-Inf 0 0 0 0 0];
37 ub=[Inf Inf Inf 1 Inf 0.9999];
38 disp('The CONSTRAINED calibration result is ([mu sigma lambda p
       etaPlus etaMinus])');
39 theta_cal_const = fmincon(distance,theta0,[],[],[],[],lb, ub,
       [], options)
40
41 disp('The calibration result is ([mu sigma lambda p etaPlus
       etaMinus])');
42 theta_cal = fminsearch(distance,theta0, options)
43
44 %% The fit is gauged by comparison to the kernel density
       estimate
```

```
45 [f_data, xi_data, bw_data] =ksdensity(log_returns, 'width',
       0.012);
46
47 addpath ../Simuleringar
48 theta_sim = theta_cal;
49 simul_ratio=1; % The simulation size is simul_ratio times the
       data size
50 simulated_log_returns = diff(levy(1, length(log_returns)*
       simul_ratio, ...
51     period_length*simul_ratio, theta_sim(1), theta_sim(2),
           theta_sim(3), ...
52     theta_sim(4), theta_sim(5), theta_sim(6)));
53 rmpath ../Simuleringar
54
55 [f_simul, xi_simul, bw_simul] =ksdensity(simulated_log_returns,
       'width', 0.012);
56
57 figs2keep = []; % The numbers of the figures to be kept
58 all_figs = findobj(0, 'type', 'figure');
59 delete(setdiff(all_figs, figs2keep));
60
61 figure(1)
62 plot(xi_data, log(f_data),'b', xi_simul, log(f_simul),'--r','
       LineWidth', 1.2);
63 legend('Kernel estimator','Kou model');
```

```
1 % FILE: characteristic_exponent.m
2
3 function [ psi_theta ] = characteristic_exponent( u, theta )
4 % CHARACTERISTIC_EXPONENT Returns the value of the
5 % characteristic exponent of the Kou model for specific u and a
       specific
6 % set of model parameters theta, as by P. Tankov
7
8 u = reshape(u,1,length(u)); % Reshape u into a row vector
9 b = theta(1); sigma = theta(2); lambda = theta(3); p = theta(4)
      ;
10 etaPlus = theta(5); etaMinus = theta(6);
11
12 psi_theta = -sigma^2*u.^2./2 + 1i*b*u + lambda*p./(1+1i*u*
       etaMinus) ...
13     + lambda*(1-p)./(1-1i*u*etaPlus) - lambda; % A row vector
14 end
```

```
% FILE: empirical_characteristic_exponent.m

function [ psi_hat ] = empirical_characteristic_exponent( u,
    log_returns, time_resolution )
% EMPIRICAL_CHARACTERISTIC_EXPONENT Returns the value of the
    empirical characteristic
% exponent for specific u, based on a set of log returns with
% time-resoultion in the unit 1 year (for daily returns
    time_resolution is
% approximately 1/252)

u = reshape(u,1,length(u)); % Reshape u into a row vector
log_returns = reshape(log_returns,length(log_returns),1); %
    Ditto

psi_hat = 1/time_resolution*log(mean(exp(1i*log_returns*u))); %
    A row vector
end
```

```
% FILE: weight.m

function [ w ] = weight( u, sigma_star )
% WEIGHT Returns the value of the weight funcion for specific u
% and sigma_star

u = reshape(u,1,length(u)); % Reshape u into a row vector

w = exp(-sigma_star^2*u.^2)./(1-exp(-sigma_star^2*u.^2)); % A
    row vector
end
```

```
% FILE: ou_calibrate_ml.m

function [mu,sigma,lambda] = OU_Calibrate_ML(S,delta)
  n = length(S)-1;

  Sx  = sum( S(1:end-1) );
  Sy  = sum( S(2:end) );
  Sxx = sum( S(1:end-1).^2 );
  Sxy = sum( S(1:end-1).*S(2:end) );
  Syy = sum( S(2:end).^2 );

  mu  = (Sy*Sxx - Sx*Sxy) / ( n*(Sxx - Sxy) - (Sx^2 - Sx*Sy) );
```

```
    lambda = -log( (Sxy - mu*Sx - mu*Sy + n*mu^2) / (Sxx -2*mu*Sx
        + n*mu^2) ) / delta;
    a = exp(-lambda*delta);
    sigmah2 = (Syy - 2*a*Sxy + a^2*Sxx - 2*mu*(1-a)*(Sy - a*Sx) +
        n*mu^2*(1-a)^2)/n;
    sigma = sqrt(sigmah2*2*lambda/(1-a^2));
end
```

D.2 Simulation code

The code used in creating the simulations is the following:

```
% FILE: main.m

clear
clc

figs2keep = [];
all_figs = findobj(0, 'type', 'figure');
delete(setdiff(all_figs, figs2keep));

%% Model parameters are set up

T = 5;
disp('The Kou model parameters used are ([mu sigma lambda p
    etaPlus etaMinus])');
param_vec = [-0.473    0.245    99.9    0.230    0.0153    0.0256] %
     Calibrated parameters
lambda = param_vec(3); p = param_vec(4); eta_plus = param_vec
    (5); eta_minus = param_vec(6);
initial_sigma = param_vec(2); average_sigma = param_vec(2);
mu = param_vec(1);

k = 20; delta = 0.9;
s0 = 1;                 % initial stock price
m0 = 3.5;               % initial multiplier of the cushion
m_final = 3.5;          % final multiblier in parameter sweep
dell = 0.1;             % Fine-ness of multiplier parameter sweep
G = 0.85;               % guaranteed amount
volatility_r = 0.02;    % volatility of the riskless interest
    rate process
r0 = 0.02;              % initial riskless interest rate
```

```
27 a = 2; b = 0.04;        % parameters of the Ornstein-Uhlenbeck
       interest rate model
28 M = 50000;              % number of Monte Carlo iterations
29 V0 = 1;                 % initial value of the portfolio
30 R = -0.3;               % R<0 is the parameter of the option
       price formula
31
32 % The partition of the time-interval [0,T] is defined by N
       partition points
33 N = 252*T; % Daily adjustments
34 h = T/N;
35 t = 0:h:T;
36
37 %% Volatility surface, Levy process realisations, stockprice-,
       riskless interest rate- and bond price evolutions are
       generated
38
39 % A volatility surface is generated
40 sigma = sigma_fct( M, N, T, k, initial_sigma, average_sigma,
       delta );
41
42 % Levy process realisations are created according to the Kou
       model
43 Z = levy( M, N, T, mu, average_sigma, lambda, p, eta_plus,
       eta_minus); %sigma instead of avg
44
45 % Stock price evolutions are computed (for graphical
       representation and OBPI)
46 stockprice = zeros(M, N+1);
47 stockprice(:,1) = s0;
48 for i=2:N+1
49     stockprice(:,i) = stockprice(:,i-1) + ...
50         stockprice(:,i-1).*(Z(:,i)-Z(:,i-1)); %First order
               Taylor expansion?
51 end
52
53 % Realisations of the evolution of the riskless interest rate
       and the bond
54 % price are generated
55 [r, bond] = bond_price( M, a, b, volatility_r, N, T, r0 );
56
57 %% CPPI STRATEGY
58
```

```
59 L = length(m0:dell:m_final);
60
61 mean_CPPI = zeros(1,L);
62 std_deviation_CPPI = zeros(1,L);
63 default_rate_CPPI = zeros(1,L);% Fraction of CPPI portfolios
       defaulting
64 average_loss = zeros(1,L); % Average loss
65 conditional_average_loss = zeros(1,L); % Average loss
       conditional on that a loss happens
66
67
68 for j=1:L
69
70     m = m0+(j-1)*dell;
71     % The cushion multiplier is estimated
72     m = m*ones(1,N); % real(m0*sigma/initial_sigma).^(-0.17);
73
74     % Further, the evolution of the CPPI portfolio value is
           computed
75     V = zeros(M, N+1);
76     zer = zeros(M, 1);
77     V(:,1) = V0;
78     risky_investment = zeros(M, N+1);
79     for i=2:N+1
80         risky_investment(:,i) = min(max(zer, m(:,i-1).*real( V
               (:,i-1) ...
81             -G*bond(:,i-1))), real(V(:,i-1)));
82         V(:,i) = V(:,i-1) + risky_investment(:,i).*(Z(:,i)-Z(:,
               i-1)) ...
83             + ((bond(:,i)-bond(:,i-1))./bond(:,i-1)).*(V(:,i-1)
                   -risky_investment(:,i));
84     end
85
86     if m0==m_final
87         figure(1)
88         plot(t, V,'b', t, stockprice,'r', t, G*ones(1,N+1),'k',
               'LineWidth', 1.2);
89         legend('CPPI portfolio value','Stock price', 'Floor');
90         xlabel('Time (years)');
91         ylabel('Stock price/Portfolio Value');
92         title('CPPI on BMW-calibrated simulated stock data');
93     end
94
```

```
95
96      % Finally, some metrics of performace are calculated
97      mean_CPPI(j) = mean(V(:, N+1)) % Mean final portfolio value
            for the CPPI strategy
98      std_deviation_CPPI(j) = std(V(:,N+1)); % Standard deviation
            of final portfolio value
99      [rr, cc, vv] = find(V(:,N+1)<G-0.0000005); % Finding
            defaulting protfolios
100     default_rate_CPPI(j) = length(vv)/M % Fraction of CPPI
            portfolios defaulting
101     vv = V(rr,N+1); % Values of defaulting portfolios
102     conditional_average_loss(j) = mean(G-vv); % Average loss
            conditional on that a loss happens
103     average_loss(j) = mean(G-vv)*length(vv)/M; % Average loss
104 end
105
106 if m0~=m_final
107     figure(1)
108     plot(m0:dell:m_final, default_rate_CPPI, 'LineWidth', 1.2)
109     grid on
110     xlabel('Multiplier');
111     ylabel('Probability of loss');
112     set(gca,'XMinorTick','on','YMinorTick','on')
113
114     figure(2)
115     plot(m0:dell:m_final, average_loss, 'LineWidth', 1.2)
116     grid on
117     xlabel('Multiplier');
118     ylabel('Average loss');
119     set(gca,'XMinorTick','on','YMinorTick','on')
120
121     figure(3)
122     plot(m0:dell:m_final, conditional_average_loss, 'LineWidth'
            , 1.2)
123     grid on
124     xlabel('Multiplier');
125     ylabel('Conditional average loss');
126     set(gca,'XMinorTick','on','YMinorTick','on')
127 end
128
129 %% OBPI STRATEGY
130
131 % The price of the European put option is calculated
```

```
132
133 % The initial investments of the OBPI portfolio
134 investment_stocks_OBPI = (V0-G*exp(-r0*T))*m0;  % Amount of
    money invested in stocks
135 number_stocks_OBPI = investment_stocks_OBPI/s0; % Total number
    of stocks (this number is final)
136 number_bonds_OBPI = (1 - number_stocks_OBPI*s0)*exp(r0*T); %
    This is simply
137     % the initial number of bonds; the final number depends on
        the put, and is calculated below
138
139 %If the number of zero-coupon bonds is smaller than the
    guaranteed amount,
140 %then the difference is used to buy puts
141 if number_bonds_OBPI<G
142     fun = @(x) put_price(T, G-x, R, r0, investment_stocks_OBPI,
        lambda, ...
143         p, eta_plus, eta_minus, average_sigma, mu) + x*exp(-r0*
            T) ...
144         + investment_stocks_OBPI - V0;
145     c0 = 0;
146     number_bonds_OBPI = fzero(fun,c0);
147 end
148
149 % The final value of the OBPI portfolio is calculated
150 value_OBPI = real(number_stocks_OBPI*stockprice + ones(size(
    stockprice,1),1)*number_bonds_OBPI*exp(-r0*(T-t)) +
    put_price(T-t, G-number_bonds_OBPI, R, r0,
    number_stocks_OBPI*stockprice, lambda, ...
151         p, eta_plus, eta_minus, average_sigma, mu));
152 figure(2)
153 plot(t, value_OBPI,'b', t, stockprice,'r',t, G*ones(1,N+1),'k',
    'LineWidth', 1.2);
154 legend('OBPI portfolio value','Stock price', 'Floor');
155 xlabel('Time (years)');
156 ylabel('Stock price/Portfolio Value');
157 title('OBPI on BMW-calibrated simulated stock data');
158
159 pp = put_price(T-t, 0.7, R, r0, stockprice, lambda, ...
160         p, eta_plus, eta_minus, average_sigma, mu);
161
162 figure(3)
```

```
plot(t, pp, t, stockprice,t, 0.75*ones(1,N+1),'k','LineWidth', 1.2);
legend('Put price','Stock price', 'Stike');
xlabel('Time (years)');
ylabel('Put/Stock price');
title('');


%Finally, some metrics of performace are calculated
mean_OBPI = mean(value_OBPI(:,N+1)); %Mean final portfolio value for the OBPI strategy
std_deviation_OBPI = std(value_OBPI(:,N+1));%/sqrt(T); % Standard deviation of final value
```

```
% FILE: levy.m

function [ Z ] = levy( M, N, T, mu, sigma, lambda, p, eta_plus, eta_minus)
% LEVY This function returns M realizations, as the matrix Z, of a Levy
% process generated according to the Kou model with the given parameters

% This Levy process is the sum of the deterministic trend mu*t, Brownian
% part sigma*B_t, and jump part sum(Y_i,1,N_t)

Z = zeros(M, N+1); Z(:, 1) = 0; h = T/N; t = (0:h:T);

% First the Brownian part is generated
brown = abs(sigma) .* normrnd(0,1,M,N+1) * sqrt(h);

% Second the jump prat is generated
jump = zeros(M, N+1);
poi = poissrnd(lambda*h,M,N); % poi(i,j) is number of jumps that occur
% within the timespace (j-1)*h to j*h for the i:th process realization
for i=1:M
    for j=2:N+1
        for k=1:poi(i,j-1)
            if rand>p
                jump(i,j) = jump(i,j) - log(rand)*eta_plus;
            else
```

```
                jump(i,j) = jump(i,j) + log(rand)*eta_minus;
            end
        end
    end
end

% Finally the trend is added, and the wanted process
    realization created
for i=2:N+1
    Z(:,i) = Z(:,i-1) + max(-0.99, mu*h + brown(:,i) + jump(:,i
        ));
    % The max(-0.99,_) restriction is applied to ensure (
        strictly) positive
    % asset prices
end
end
```

```
% FILE: bond_price.m

function [ r, bond ] = bond_price( M, a, b, sigma, N, T, r0 )
%BOND_PRICE This function calculates the evolution of the
    riskless interest rate and
%the bond price. It is assumed that the interest rate follows
    the Ornstein
%Uhlenbeck process with volatility sigma

r = zeros(M, N+1);
bond = zeros(M, N+1);
h = T/N;

%The initial values of the interest rate and bond price are set
r(:,1) = r0;
bond(:,1) = exp(-r0*T);

%In order to avoid discretization errors, the closed form
    solutions for the
%interest rate and bond price are used
integr = sqrt(integral(@(s) exp(2*a*s), 0, h));
for i=2:N+1
    r(:,i) = r(:,i-1)*exp(-a*h) + b*(1-exp(-a*h)) + sigma*exp(-
        a*h)*integr*normrnd(0,1,M,1);
    bond(:,i) = exp(-b*(T-(i-1)*h) + (b-r(:,i))*(1-exp(-a*(T-(i
        -1)*h)))/a ...
        - (sigma^2/(4*a^3))*(1-exp(-a*(T-(i-1)*h)))^2 ...
```

```
23          + (sigma^2/(2*a^2))*(T-(i-1)*h-(1-exp(-a*(T-(i-1)*h)))/
                a));
24  end
25  end
```

```
1  % FILE: sigma_fct.m
2
3  function [ sigma ] = sigma_fct( M, N, T, k, initial_sigma,
       average_sigma, delta )
4  %SIGMA_FCT This function returns M realisations, as the matrix
       sigma, of a
5  %stochastic volatility process with the given parameters
6
7  sigma = zeros(M, N+1);
8  sigma(:,1) = initial_sigma;
9  h=T/N;
10 brownian_increments = sqrt(h)*normrnd(0,1,M,N);
11 for i=2:N+1
12     sigma(:,i) = sigma(:,i-1) + k*(average_sigma - sigma(:,i-1))
           *h + delta*sqrt(sigma(:,i-1)).*brownian_increments(:,i-1)
           ;
13 end
14 end
```

```
1  % FILE: put_price.m
2
3  function x = put_price(T, K, R, r0, stockprice, lambda, p,
       eta_plus, eta_minus, sigma, mu)
4  % PUT_PRICE Calculates the price of a European put option with
       time to maturity
5  % T and strike K, given the intial stock price and that the
       price dynamic
6  % follows the exponential Levy process
7
8  T_mat = ones(size(stockprice,1),1)*T;
9  kf=log(K./stockprice)-r0.*T_mat; % log-forward moneyness
10
11 % The integrand function is defined as per Appendix B
12 u1 = @(x) x - 1i*R;
13 integrand = @(u) exp(1i.*u.*kf + 1i.*u1(u).*T_mat.*mu-0.5*sigma
       ^2 * u1(u).^2*T_mat + ...
14      T_mat*lambda*(p./(1+1i*u1(u)*eta_minus) + (1-p)./(1-1i*u1(u
            )*eta_plus)-1))./((R-1i*u).*(R-1-1i*u));
15
```

```
16 % Finally, the integration is carried out
17 x = stockprice.*exp(kf.*(1-R)).*real(integral(integrand,-50,
       50, 'ArrayValued',true))/(2*pi);
18 end
```